

Computer simulation – a tool for optimisation of ventilator setting in critical lung disease

AKADEMISK AVHANDLING

som med vederbörligt tillstånd av Medicinska fakulteten vid Lunds universitet för avläggande av doktorsexamen i medicinsk vetenskap kommer offentligen att försvaras i Föreläsningssal 1, Universitetssjukhuset i Lund, onsdagen den 11 december 2002 kl 09.00

av

Leif Uttman

Medicine kandidat

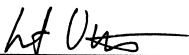
Fakultetsopponent:
Professor Göran Hedenstierna
Uppsala universitet

Organization LUND UNIVERSITY Department of Clinical Physiology University Hospital SE-221 85 Lund	Document name DOCTORAL DISSERTATION	
	Date of issue 2002-12-11	
	Sponsoring organization Swedish Research Council (No 02872) Swedish Heart-Lung Foundation Faculty of Medicine, Lund University, Sweden	
Author(s) Leif Uttman		
Title and subtitle Computer simulation - a tool for optimisation of ventilator setting in critical lung disease		
Abstract Increasing attention is paid to mechanical ventilation as one cause behind aggravation of lung injury. Lung protective ventilation can be achieved e.g. by minimising tidal lung collapse and re-expansion and by the use of small tidal volume allowing some degree of permissive hypercapnia. The ventilator and the sick lung comprise a very complex system. Identification of a ventilator setting that with respect to respiratory rate, tidal volume, I:E ratio, PEEP, etc is optimal with respect to desired physiological effects is therefore difficult. The main objective behind this thesis was to develop and validate a system for computer simulation of respiratory mechanics and gas exchange that allows prediction of physiological effects of resetting the ventilator. To reach this objective, methods for characterisation of lung physiology, which require little or no disturbance of the breathing pattern, were developed. Complementary studies of how gas exchange is affected by ventilator setting were performed. Longer time for equilibration between inspired and alveolar gas decreased airway dead space. When, in acute lung injury, PaO ₂ increased in response to PEEP alveolar dead space decreased and vice versa. The hypothesis that mechanical behaviour and CO ₂ elimination after resetting respiratory rate and tidal volume could be predicted by simulation in healthy pigs was confirmed. Further, the hypothesis that immediate effects of moderate PEEP increments on mechanics and CO ₂ elimination in patients with acute lung injury could be predicted by simulation was also confirmed. Future development of the lung model used for simulation was outlined so as to include how time for gas equilibration affects gas exchange and to account for non-linear elastic properties. Iterative simulation may be a tool in future goal-oriented ventilation strategies.		
Key words: (MeSH): Computer Simulation · Artificial Respiration · Pulmonary Gas Exchange · Respiratory Dead Space · Respiratory Mechanics · Respiratory Distress Syndrome, Adult · Swine		
Classification system and/or index terms (if any):		
Supplementary bibliographical information:		Language English
ISSN and key title:		ISBN 91-628-5443-7
Recipient's notes	Number of pages	Price
	Security classification	

Distribution by (name and address)

I, the undersigned, being the copyright owner of the abstract of the above-mentioned dissertation, hereby grant to all reference sources permission to publish and disseminate the abstract of the above-mentioned dissertation.

Signature



Date

2002-10-30

Computer simulation – a tool for optimisation of ventilator setting in critical lung disease

Leif Uttman

Department of Clinical Physiology, Lund
Lund University, Sweden
2002



LUND
UNIVERSITY

© Leif Uttman 2002

Department of Clinical Physiology, Lund
Lund University, Sweden

ISBN 91-628-5443-7
Printed by KFS AB, 2002

Contents

LIST OF PAPERS

ABBREVIATIONS

1. BACKGROUND	9
2. OBJECTIVES	15
3. PAPERS	16
4. MATERIAL AND METHODS.....	17
4.1 SUBJECTS.....	17
4.2 MUSCLE RELAXATION, ANAESTHESIA AND SEDATION	17
4.3 MECHANICAL VENTILATION	17
4.4 EQUIPMENT FOR DATA ACQUISITION AND ANALYSIS	17
4.5 RECORDINGS	18
4.6 DATA ANALYSIS	18
4.7 COMPUTER SIMULATION	22
5. RESULTS AND DISCUSSION.....	23
5.1 CONCEPTUAL ACHIEVEMENTS	23
5.2 LIMITATIONS	24
5.3 CONCLUDING REMARKS	29
6. ACKNOWLEDGEMENTS.....	30
7. SAMMANFATTNING	31
8. REFERENCES	32

LIST OF PAPERS

The thesis is based on the following papers, which are referenced in the text by their Roman numerals.

- I. Leif Uttman & Björn Jonson**
Computer-aided ventilator resetting is feasible on the basis of a physiological profile
Acta Anaesthesiol Scand. 2002;46:289–296
- II. Laurent Beydon, Leif Uttman, Ravi Rawal & Björn Jonson**
Effects of positive end-expiratory pressure on dead space and its partitions in acute lung injury
Intensive Care Med. 2002;28:1239–1245
- III. Leif Uttman & Björn Jonson**
A prolonged post-inspiratory pause enhances CO₂ elimination by decreasing airway dead space
Submitted for publication
- IV. Leif Uttman, Laurent Beydon & Björn Jonson**
Effects of PEEP increments can be predicted by computer simulation based on a physiological profile in acute lung injury
Submitted for publication

Abbreviations

ALI: acute lung injury

ARDS: acute respiratory distress syndrome

C: compliance of the respiratory system

g_0 and g_1 : coefficients for the description of linear expiratory conductance

I:E ratio: inspiratory:expiratory ratio

MDT: mean distribution time

P_{CO_2} : partial pressure of CO_2 in the airway

$P_{CO_2,A}$: alveolar partial pressure of CO_2

$P_{CO_2,ET}$: end-tidal partial pressure of CO_2

PEEP: positive end-expiratory pressure

P_{el} : elastic recoil pressure of the respiratory system

$P_{el,E}$: post-expiratory elastic recoil pressure

P_{peak} : peak airway pressure

$P_{plateau}$: post-inspiratory plateau pressure

P_{tr} : tracheal pressure

P_{vent} : pressure in the ventilator

R_E : expiratory resistance

R_I : inspiratory resistance

RR: respiratory rate

V: volume

$V_{CO_2,E}$: volume of CO_2 expired with each breath

$V_{CO_2,I}$: volume of CO_2 re-inspired with each breath

$V_{CO_2,T}$: tidal CO_2 elimination

V_D : dead space

$V_{Daw,dist}$: airway dead space distal to the CO_2 sensor

$V_{Daw,prox}$: airway dead space proximal to the CO_2 sensor

$V_{Daw,tot}$: total airway dead space

V_{Dphys} : physiological dead space

V_E : volume expired

V_T : tidal volume

$V_{T,alt}$: alternative tidal volume

VALI: ventilator-associated lung injury

\dot{V}_{aw} : airway flow

\dot{V}_{CO_2} : CO_2 elimination per minute

1. Background

Mechanical ventilation is required when a patient is unable to achieve adequate ventilation and thereby gas exchange. This may occur under many circumstances, for example in connection with surgery when heavy anaesthesia and paralysis suppress the ventilation, or in acute respiratory failure caused by exacerbation of chronic obstructive pulmonary disease, acute lung injury (ALI) or acute respiratory distress syndrome (ARDS). The traditional way of delivering mechanical ventilation is through a tube that is passed into the trachea with its tip located distal to the vocal cords but proximal to the tracheal bifurcation. A rising pressure in the ventilator's inspiratory line forces volume into the patient. The passive expiration follows from a sudden drop in airway pressure. The ventilation pattern must be adapted to suit the patient's need for CO₂ elimination (\dot{V}_{CO_2}) and oxygenation. \dot{V}_{CO_2} is adjusted by changing the volume given to the patient each minute. Oxygenation is secured by delivering adequate ventilation, keeping the lungs "open", and adjusting the oxygen content of inspiratory air. Systems for patient-ventilator interaction have been developed to allow different degrees of ventilation support.

Increasing attention has been paid to the role of mechanical ventilation in the aggravation of lung injury denoted ventilator-associated lung injury (VALI). Different types of trauma have been identified during mechanical ventilation:

Barotrauma: gas leakage into the extra-alveolar space, traditionally associated with high airway pressure. In general it is anticipated that it is peak pressure rather than mean or positive end-expiratory pressure (PEEP) that is harmful (1). However, absolute pressure in itself is not dangerous as trumpet players may reach airway pressures of 150 cm H₂O numerous times per day without developing lung injury (2). Instead, the differential pressure over a lung unit leading to regional overdistention has been suggested to be the critical feature (3, 4).

Volutrauma: regional lung overdistention caused by high end-inspiratory lung volumes in combination with mechanical heterogeneity of lung units (3).

Atelectrauma: lung damage that results from collapse and re-expansion repeated breath by breath. Healthy lungs tolerate such a process thousands of times (5). However, after perturbation of surfactant function the lung becomes vulnerable to repeated opening and closing (6). This is considered to reflect shear forces between expanded and collapsed lung zones (4, 7, 8).

Biotrauma: activation of inflammatory mechanisms due to the physical stress of mechanical ventilation (9).

Oxytrauma: detrimental effects of high concentration of oxygen in the inspired gas due to reactive oxygen species (10). However, in patients with ALI/ARDS the relative tolerance to high concentration of oxygen may be increased (11).

These different types of trauma often occur together and are interdependent. For example, volutrauma and barotrauma are difficult to separate (3). In sepsis, biotrauma in terms of inflammation may lead to protein leakage into the alveolar space, surfactant inactivation and atelectrauma. On the other hand, atelectrauma may lead to biotrauma (12).

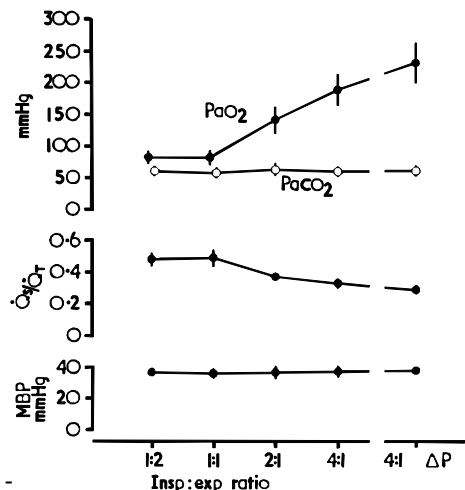
The alveolo-capillary membrane over which gas exchange occurs has an important role in preventing free passage of many molecules. It consists of endothelium, interstitium, alveolar epithelium and a film of surfactant. This film has been proposed to prevent permeability of water-soluble molecules and not only to reduce surface tension (13, 14). Experimental perturbation of the surfactant film by administration of detergent (dioctyl sulphosuccinate) causes exchange of albumin between plasma and the alveolar space by a different mechanism compared to that of large tidal volume (V_T) ventilation (15, 16). When the alveolo-capillary membrane is damaged, as is the case in ARDS, leakage of plasma proteins leads to inactivation of surfactant. This may in turn increase the alveolo-capillary

permeability causing a vicious circle of more fluid and protein leakage into the alveolar space (6, 17, 18). In a wider perspective, surfactant inactivation increases the risk for collapse of small airways and alveoli due to increased surface tension as discussed already in 1967 by Ashbaugh and colleagues (19).

ARDS was first described in 1967 by Ashbaugh and colleagues as a syndrome with close resemblance to the infantile respiratory distress syndrome (19). ARDS included tachypnoea, severe dyspnoea, cyanosis despite oxygen therapy, decrease in respiratory system compliance, diffuse alveolar infiltration on X-ray, and microscopic appearance of hyaline membranes. A common mechanism of lung injury among the diverse groups of patients was postulated: “The loss of compliance, refractory cyanosis, and microscopic atelectasis point to alveolar instability as a likely source of trouble” (19). The use of PEEP was found to improve oxygenation by a suggested effect on alveolar stability. To this day this description of ARDS is considered valid.

Reynolds was a pioneer when he treated infants suffering from respiratory distress syndrome with pressure-controlled ventilation and inverse inspiratory:expiratory (I:E) ratio (20). He reasoned that PaO_2 will increase when using inverse I:E ratio ventilation because the alveoli will remain open for a longer proportion of each breath. Indeed, this was the case in these infants (Figure 1, upper panel). Note also the reduction in right-to-left shunt (middle panel) and the constant mean arterial pressure (lower panel).

Figure 1. Reproduced from Archives of Disease in Childhood, 1971;46:152–159, with permission from the BMJ Publishing Group. Effects of inspiratory:expiratory ratio on PaO_2 , $PaCO_2$ (upper panel), right-to-left shunt (middle panel) and mean arterial blood pressure (lower panel). ΔP shows the effect of a 5 cm H_2O increment in peak airway pressure at inspiratory:expiratory ratio 4:1.



Today, ventilation in ALI/ARDS is focused on preventing cyclic opening and closing of atelectatic alveoli by the use of PEEP and low V_T (21–23). However, five clinical trials testing low V_T in ALI/ARDS have not come to uniform results (21, 23–26). In a recent metaanalysis of these trials it is concluded that the diverging results can be attributed to significant differences in control arms (27). Consequently, we still do not know to what extent V_T has to be reduced in order to avoid VALI.

Low V_T strategies may induce hypercapnia, particularly since the fraction of ventilation that reaches the alveoli decreases when dead space (V_D) ventilation increases. It has been suggested that hypercapnia may be an acceptable consequence in the trade-off between low V_T and gas exchange (permissive hypercapnia) (28). Laffey and Kavanagh express that “future therapeutic goals might be expressed as: *keep the PaCO₂ high; if necessary, make it high; and above all, prevent it from being low*” (29). Although this group advocates a cautious use of hypercapnia, Kavanagh issues warnings against serious effects on for instance intracranial pressure and pulmonary vascular resistance (30), as do Kregenow and Swenson (31). In addition, recent studies show that permissive hypercapnia increases right-to-left shunt (32, 33).

The issue regarding clinical use of permissive hypercapnia is still not settled. In any case, CO₂ produced by metabolism must be eliminated in ways as non-deleterious as possible. There is ample experimental evidence that the use of ultra-low V_T is efficient with respect to gas exchange. Examples are extra-corporeal CO₂ removal (34), high frequency jet ventilation (35, 36), high frequency oscillation (37). However, despite promising studies in animals and infants (38–43) these techniques have not been generally accepted (44). A major obstacle may be that traditional concepts of how to set the ventilator cannot be applied (45, 46). There is evidently a need for a mode of ventilation, which allows the physician to think and act on the basis of V_T , respiratory rate (RR), PEEP and other basic features of ventilation. A step in the direction of low V_T is offered by techniques allowing reduction in V_D , for instance by using active humidifiers, tracheal gas insufflation or aspiration of V_D (47–49).

The ideal ventilator setting in ARDS is still unknown. Many ask for an optimal value of for instance V_T , RR, PEEP and post-inspiratory plateau pressure (P_{plateau}). Luciano Gattinoni expressed his view on this topic: “There are no magic numbers” (15th European Society of Intensive Care Medicine Annual Congress, Barcelona 2002). Recently Dreyfuss and Saumon advocated “Fuzzy Logic” in the treatment of critically sick patients (50): This means that a physician must create in his mind an image of the total situation of the patient. Important elements of that image are based on efficient monitoring and diagnostic measures reflecting lung function with respect to both mechanics and gas exchange. On the basis of wide knowledge about the disease and about physiology he should then apply his judgement to decide upon ways to treat. Probably most trained physicians agree that some rules apply and that these rules need to be expressed in numbers, which, if not magic, express physiological goals of treatment relevant for the specific patient. Examples of reasonable goals to maintain gas exchange and avoid VALI are:

- Reduce V_T as much as possible
- Limit P_{plateau} to 30 cm H₂O
- Maintain a high total PEEP ($PEEP_{\text{tot}}$)
- Ventilate to maintain a pH of 7.2

The suitable level of P_{plateau} and $PEEP_{\text{tot}}$ should be judged on the basis of estimates or measurements of intrathoracic/abdominal pressure that modifies the transpulmonary pressure. A pH of 7.2 may be regarded as dangerously low in many patients. Therefore, care must be taken in selected patient groups to avoid the potential danger of hypercapnic acidosis (30, 31).

Compared to many classical and recent studies it is time to widen the perspective rather than to focus on optimising single ventilator parameters such as PEEP (51), RR (52) and I:E ratio (53). An optimum ventilation pattern may depend upon V_T , RR, PEEP, I:E ratio, post-inspiratory pause time, inspiratory flow pattern and

inspiratory fraction of oxygen. Obviously, without efficient tools it is difficult or impossible to identify the optimal combination of all these ventilator settings.

In technical areas, simulation is a standard principle used to foresee what will be the effects of a particular action taken to influence a complex physical system. Furthermore, iterative simulation may be performed in order to identify an action or a combination of actions that will lead to predefined desired effects. In medicine, simulation has been recognised as an important tool, for instance when studying peritoneal fluid transport (54). Moreover, different patterns of mechanical ventilation have been simulated on the basis of mathematical lung modelling (55).

2. Objectives

The main objective was to develop and validate a system for computer simulation of respiratory mechanics and gas exchange that allows prediction of physiological effects of resetting the ventilator in intensive care. To reach this objective, methods for characterisation of lung physiology, which require little or no disturbance of the breathing pattern, were developed. Complementary studies of how gas exchange is affected by ventilator setting were performed in order to increase the knowledge in this field.

3. Papers

Paper I: Describes data analysis of mechanical properties of the respiratory system and parameters related to \dot{V}_{CO_2} yielding a physiological profile. A computer simulation program based on the profile was presented. Simulated values of airway pressures and \dot{V}_{CO_2} were validated against measured values at alternative settings of RR and V_T in healthy pigs. The study also contributes to the knowledge of respiratory physiology of pigs.

Paper II: The effects of PEEP on respiratory mechanics and gas exchange were studied in ALI. The results contribute to the knowledge of how PEEP alters respiratory physiology, particularly with respect to partitions of V_D .

Paper III: Time-dependent effects of gas mixing and diffusion on V_D and \dot{V}_{CO_2} were studied by changing the post-inspiratory pause time. The results may motivate an extension of the physiological profile.

Paper IV: Simulated values of airway pressures and \dot{V}_{CO_2} were validated against measured values at alternative PEEP levels in ALI. PEEP resetting in patients with complex physiology was considered to be a particularly difficult test situation.

4. Material and Methods

4.1 Subjects

Papers I and III include small healthy pigs of the Swedish native breed (body weight circa 30 kg). Papers II and IV include consecutive patients admitted to the intensive care unit for the reason of ALI.

4.2 Muscle relaxation, anaesthesia and sedation

Both animal and human subjects received muscle relaxants throughout the study period in order to eliminate muscle forces acting on the respiratory system. The animals were anaesthetised using a previously established protocol. The human subjects were sedated according to the routines at the intensive care unit. No anaesthetic gases were used. The animals were ventilated with air (21% oxygen) while the patients received 100% oxygen.

4.3 Mechanical ventilation

All subjects were oro-tracheally intubated and ventilated with a square-wave inspiratory flow in the supine position. In the animals, a recruitment manoeuvre was performed to standardise conditions by reducing airway closure and atelectasis. In the human subjects, no recruitment manoeuvre was performed, as the intention was to study physiology at unperturbed ventilation.

4.4 Equipment for data acquisition and analysis

The Servo Ventilator 900C and the mainstream CO₂ Analyzer 930 (Siemens-Elma, Solna, Sweden) were used in all studies. The analogue signals from built-in sensors for pressure and flow in the ventilator and the CO₂ signal were sampled by a computer at the frequency 50 Hz. Flow, pressure and CO₂ signals had a 50% response time of 12 ms and were synchronous within 8 ms (56). A spreadsheet (Excel 97, Microsoft, WA, USA) was used for analysis of all data.

4.5 Recordings

Normal breaths were recorded before and after ventilator resetting. In the study described in paper I, breaths with manual post-inspiratory and post-expiratory pauses were recorded as well.

4.6 Data analysis

Mechanics

Flow and volume signals were calibrated to BTPS conditions. Resistance of the connecting system (R_{tube}) including that of the Y-piece, CO₂ transducer connector, humidifying filter [II, IV] and the tracheal tube was considered flow dependent (turbulent flow). Coefficients defining resistance were determined *in vitro* according to the equation of Rohrer (57). This equation was also applied for the determination of resistance of the expiratory line of the ventilator at fully open PEEP valve. Tube compliance, mainly reflecting gas compression, was also measured. Airway flow (\dot{V}_{aw}) was calculated by correcting for tube compliance. Volume (V) was calculated relative to end-expiratory volume by integration of \dot{V}_{aw} . The expiratory flow signal was normalised by the use of a correction factor so that, at steady state, expired V_T equalled inspired V_T .

A mathematical lung model was defined prior to data analysis. As a goal was to develop clinically useful methods, the model should only incorporate features that can easily be studied with techniques available at the bedside. To fulfil this prerequisite, a mechanical model without hysteresis, viscoelasticity and inertia was employed. Furthermore, constant values for compliance of the respiratory system (C) and inspiratory resistance (R_I) were applied on the basis of prior data (58, 59). Expiratory resistance (R_E) was considered to vary non-linearly with V, corresponding to that conductance varies linearly with V (60).

P_{plateau} and post-expiratory elastic recoil pressure ($P_{\text{el,E}}$) were measured 0.3 s after flow cessation during the manual post-inspiratory and post-expiratory pause, respectively [I]. C was calculated as $V_T/(P_{\text{plateau}}-P_{\text{el,E}})$. In the subsequent studies P_{plateau} was measured at preset post-

inspiratory pause and C was derived from the slope of the calculated tracheal pressure (P_{tr}) versus V [II, IV]. Thereby mechanics could be determined without any intervention. Conductance was calculated as $\dot{V}_{aw}/(P_{tr}-V/C)$. For each respiratory phase a linear regression of conductance over the volume range from 15 to 85% of V_T was made, thus avoiding the influence from fast accelerations and decelerations at flow transitions. R_I was calculated from the conductance at mid- V_T [I] or as average $(P_{tr}-V/C)/\dot{V}_{aw}$ [II, IV]. R_E was calculated as $1/(g_0+g_1 \cdot V)$, where g_0 and g_1 were determined from the linear regression of expiratory conductance.

Gas exchange

V_D partitions were expressed in percent of V_T . Signals for \dot{V}_{aw} and partial pressure of CO_2 in the airway (P_{CO_2}) were analysed to yield the single breath test for CO_2 (SBT- CO_2) (Figure 2, upper panel) (61). The loop depicting P_{CO_2} versus volume (area A) reflects tidal CO_2 elimination ($V_{CO_2,T}$). Hence, physiological V_D (V_{Dphys}) was defined as:

$$V_{Dphys} = \frac{100 \cdot (PaCO_2 \cdot V_T - \text{area A})}{PaCO_2 \cdot V_T} \quad \text{Eq. 1}$$

Airway V_D distal to the CO_2 sensor ($V_{Daw,dist}$) was determined according to an algorithm of Wolff and Brunner (62). This method was modified [II, III] to correct for a sloping alveolar plateau (63) in accordance with principles previously described (64). CO_2 re-inspired from proximal airway V_D ($V_{Daw,prox}$) corresponds to area B (Figure 2) [II].

$$V_{Daw,prox} = \frac{100 \cdot \text{area B}}{PaCO_2 \cdot V_T} \quad \text{Eq. 2}$$

Alveolar V_D (V_{Dalv}) is the difference between V_{Dphys} and total airway V_D :

$$V_{Dalv} = V_{Dphys} - (V_{Daw,prox} + V_{Daw,dist}) \quad \text{Eq. 3}$$

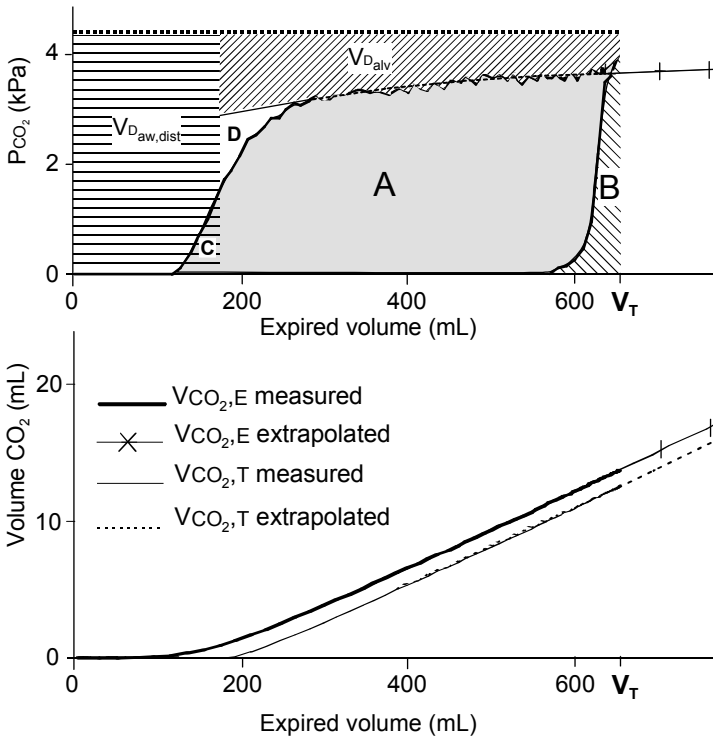


Figure 2. Modified from paper I and II.

Upper panel: In the single breath test for CO_2 the amount of CO_2 eliminated with each breath ($V_{\text{CO}_2,\text{T}}$) corresponds to area A within the loop depicting P_{CO_2} versus volume. Airway dead space distal to the CO_2 sensor is indicated by the horizontally hatched area ($V_{\text{Daw,dist}}$). Airway dead space proximal to the sensor is indicated by hatched area B representing re-inspired CO_2 ($V_{\text{CO}_2,\text{I}}$). Alveolar dead space is illustrated by the hatched area marked V_{Dalv} between the extrapolated alveolar plateau (thin line) and PaCO_2 (heavy interrupted line). The mode of calculation of V_{Dalv} implies that the triangles C and D are of equal size. The crossed line indicates the extrapolated alveolar plateau.

Lower panel: The heavy and crossed lines represent integration of the information in upper panel yielding $V_{\text{CO}_2,\text{E}}$ (areas A+B) as a function of volume. Thin and dotted lines represent $V_{\text{CO}_2,\text{T}}$ obtained by subtraction of $V_{\text{CO}_2,\text{I}}$ from $V_{\text{CO}_2,\text{E}}$.

To determine how $V_{CO_2,T}$ would vary with V_T the SBT- CO_2 was further analysed. The alveolar plateau ($P_{CO_2,A}$), describing how P_{CO_2} varies during late expiration, was expressed according to Eq. 4 (63, 65). The equation was applied over the last 40% of expired volume (V_E).

$$P_{CO_2,A} = f_0 + f_1 \cdot \ln(V_E) \quad \text{Eq. 4}$$

$V_{CO_2,T}$ needed to be segmented into expired volume of CO_2 ($V_{CO_2,E}$, areas A+B) and re-inspired volume of CO_2 ($V_{CO_2,I}$, area B) [I]. How $V_{CO_2,E}$ would vary with V_T was calculated by integration of Eq. 4 (Figure 2, lower panel). How $V_{CO_2,I}$ would vary with V_T was calculated on basis of the assumption that area B is proportional to end-tidal P_{CO_2} ($P_{CO_2,ET}$) as described by $P_{CO_2,A}$ at V_T (Eq. 4).

$V_{CO_2,E}$, $V_{CO_2,I}$, $P_{CO_2,ET}$, f_0 , f_1 , C , R_I , g_0 and g_1 together with corresponding equations mathematically characterise lung function and thus define the physiological profile of the subject.

The physiological profile did not include time-dependent effects of gas mixing and diffusion on $V_{CO_2,T}$. In paper III these aspects were studied. Mean distribution time (MDT) was defined as the mean time given to inspired gas for distribution and diffusive mixing within the lungs. For a certain pattern of inspiration, including the post-inspiratory pause, MDT was calculated from all samples during a recorded inspiration as:

$$MDT = \frac{\sum(\dot{V}_{aw} \cdot t_{dist})}{\sum \dot{V}_{aw}} \quad \text{Eq. 5}$$

t_{dist} is the time left for distribution of the particular gas sample until start of expiration.

Averages or medians of all analysed parameters from 10 recorded breaths were calculated. Irregular breaths were discarded.

4.7 Computer simulation

The simulation process mimics volume-controlled ventilation by keeping the simulated inspiratory flow rate constant, and during expiration, by not allowing pressure in the ventilator (P_{vent}) to fall below PEEP. During early expiration P_{vent} is higher than PEEP. This prevails as long as ventilator resistance at fully open expiratory valve multiplied by expiratory flow is higher than PEEP.

Mathematical simulation of ventilator function was stepwise performed by dividing the respiratory cycle into short time intervals. During each interval P_{vent} , P_{tr} and elastic recoil pressure (P_{el}), \dot{V}_{aw} and V were calculated. The basic time interval used in the simulation was 1% of the breathing cycle so as to divide the breath into 100 intervals. In order to avoid oscillations at sudden pressure and flow changes the time interval during phase transitions was reduced. For the same reason, filtering of R_{tube} , P_{vent} and expiratory \dot{V}_{aw} was performed.

During inspiration, \dot{V}_{aw} was determined by V_T , RR and inspiratory time. V was obtained as the integral of \dot{V}_{aw} . P_{el} was calculated as V/C and P_{tr} was calculated as $P_{vent} - \dot{V}_{aw} \cdot R_{tube}$. During expiration, \dot{V}_{aw} was calculated as:

$$\dot{V}_{aw} = \frac{P_{el} - P_{vent}}{R_E + R_{tube}} \quad \text{Eq. 6}$$

Six consecutive breaths were simulated. Simulated values of peak airway pressure (P_{peak}), P_{tr} , $P_{plateau}$ and \dot{V}_{CO_2} at the 6th simulated breath were compared to the average [I] or median recorded values [IV] from 10 breaths starting 30 s and 10 minutes after resetting.

5. Results and Discussion

5.1 Conceptual achievements

Dreyfuss and Saumon denote the prevailing approach to set ventilators as “cook-book medicine”, according to which patients should be ventilated with particular values of for instance PEEP and V_T (50). They suggest that we should rather use “our intellect and limited knowledge ... and reason with our natural ‘fuzzy logic’, the only way to approach the solving of an equation with so many ill-defined variables”. We suggest that the physician should, on the basis of all available information, define the physiological goals or endpoints for mechanical ventilation using the ‘fuzzy logic’ approach as suggested by Dreyfuss and Saumon. This concept may be denoted “Goal-Oriented Ventilation”. However, if the goals as well as the properties of the respiratory system are mathematically defined we consider it possible to use a physical and mathematical approach in setting the ventilator rather than fuzzy logic.

Accordingly, the ultimate aim of the present project is to offer clinicians a completely new approach to set ventilators in critical lung disease. The studies behind this thesis represent the initial steps in that direction. It is obvious that goals of ventilation cannot be described only in terms of mechanics or gas exchange, but as a combination of these. Oxygenation depends upon several physiological factors, which can be studied bedside only with invasive and complex methods. Examples are cardiac output, right-to-left shunt and ventilation/perfusion non-homogeneity, which are not easily measured. The process behind oxygenation can therefore not be subject to simulation. In this thesis focus is on \dot{V}_{CO_2} and mechanics.

The hypothesis that mechanical behaviour and \dot{V}_{CO_2} after resetting RR and V_T could be predicted by simulation in healthy pigs was confirmed [I]. Further, the hypothesis that immediate effects of moderate PEEP increments on mechanics and \dot{V}_{CO_2} in patients with ALI could be predicted by simulation was also confirmed [IV].

5.2 Limitations

The lung model includes considerable simplifications:

Absence of hysteresis between inspiratory and expiratory limbs of the P_{el}/V loop was assumed. Over a volume range not larger than an ordinary V_T , static hysteresis is not significant in patients without lung disease (66), nor in patients with critical lung disease (67). In healthy rabbits this was the case even over an extended volume range (59).

To measure viscoelastic properties takes complex breathing manœuvres. These properties were therefore not included in the model. However, measured pressure includes the pressure component related to viscoelastic impedance. Viscoelastic properties will therefore contribute to the calculated values for resistance and elastance. The “partition of viscoelastic impedance” between resistance and elastance will in a complex way depend on RR, flow waveform and viscoelastic properties. It was assumed that the model limitation with respect to viscoelastic properties would not induce significant errors. The absence of systematic differences between simulated and measured pressures [I], when RR and V_T were changed, supports this assumption.

A linear elastic property of the respiratory system was defined by a constant C . In healthy pigs [I], predicted values of P_{peak} and $P_{plateau}$ deviated from measured values with less than 1 cm H₂O (95% confidence). This is to be expected as long as the P_{el}/V relationship is nearly linear. On the contrary, large simulation errors are to be expected when the P_{el}/V curve is substantially non-linear. This is the case in patients with critical lung disease ventilated with PEEP (67). Nevertheless, simulation errors of P_{peak} , $P_{plateau}$ and mean tracheal pressure were non-significant or trivial when PEEP was increased from 0 up to 10 cm H₂O in ALI [IV]. The likely explanation for this positive result is as follows. As expected, C declined with PEEP. A lower C implied a shorter time constant for the exponentially falling lung volume and therefore a faster emptying of the lungs. Therefore $PEEP_{tot}$ fell. Then, inspiration started at lower values of P_{el} as confirmed by our measurements (Figure 3). Overall, the lower $PEEP_{tot}$

compensated for the lower C resulting in non-significant simulation errors in P_{peak} and P_{plateau} for PEEP increments up to 10 cm H₂O.

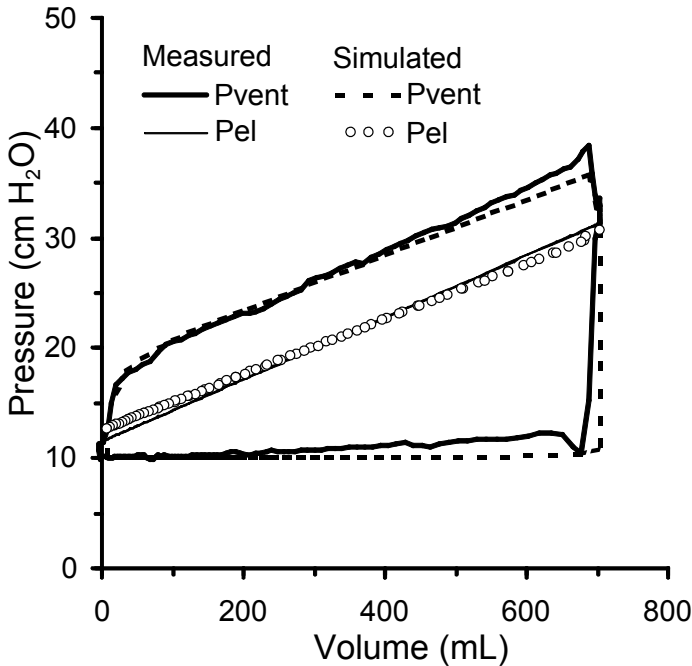


Figure 3. Measured and simulated pressure/volume loops of ventilator pressure (P_{vent}) and elastic recoil pressure (P_{el}).

Previous observations in critical lung disease show linear elastic properties within the V_T range when no PEEP is applied and non-linear properties at PEEP (67). This implies that a more complex model may be motivated when studying elastic properties at PEEP. The non-linear model suggested by Ranieri and co-workers (68) is then a better alternative. In fact, we use this model in an ongoing study of optimisation of mechanical ventilation in experimental ARDS.

R_I was considered to be constant (66, 69, 70). However, over a wide volume range R_I decreased by nearly 50% in ALI patients [II]. This may be explained by altered radius of small airways caused by interdependence between these and alveoli. Airway radius has an

immense effect on resistance – at laminar flow, doubling the radius gives 16 times higher flow (Poiseuille’s law).

In the model, R_E was assumed to vary with volume. Indeed, measured R_E decreased with volume [II]. In contrast to what is the case during inspiration, dynamic compression and airway collapse may cause an increase in R_E during expiration. This may explain the pronounced increase in R_E during late expiration at PEEP 0 [II] (Figure 4, upper panel). However, at very high volumes (PEEP 15) R_E was higher at the beginning than at the end of expiration (Figure 4, lower panel). This may be explained by longitudinal stretch that at overdistention leads to decreased airway radius (67, 71).

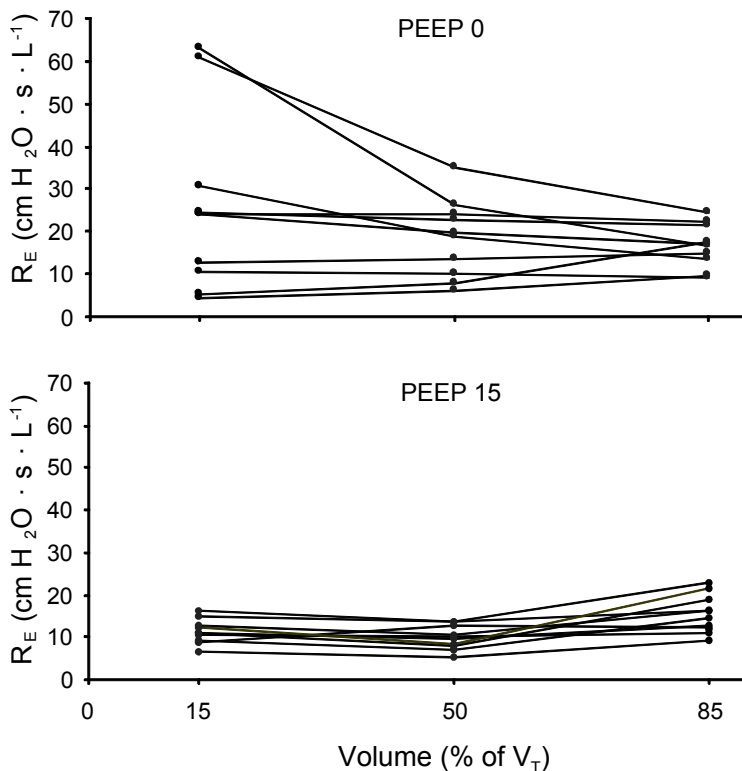


Figure 4. Modified from paper II. Expiratory resistance (R_E) at the beginning, middle and end of expiration in each subject, at 0 end expiratory pressure (PEEP 0, upper panel) and at 15 positive end-expiratory pressure (PEEP 15, lower panel).

Inertia caused by acceleration or retardation of gas is only important at flow transitions and was not modelled.

How V_D might vary in response to PEEP and MDT changes was not modelled because of limiting prevailing knowledge. When PEEP was increased from 0 up to 15 cm H₂O, simulation significantly overestimated \dot{V}_{CO_2} by up to 11% in ALI patients [IV]. It was quite surprising that $V_{D_{phys}}$ did only change slightly with PEEP in a subgroup (10/12) of these patients [II] (Figure 5). Unaffected $V_{D_{phys}}$ was reflected in a nearly constant PaCO₂.

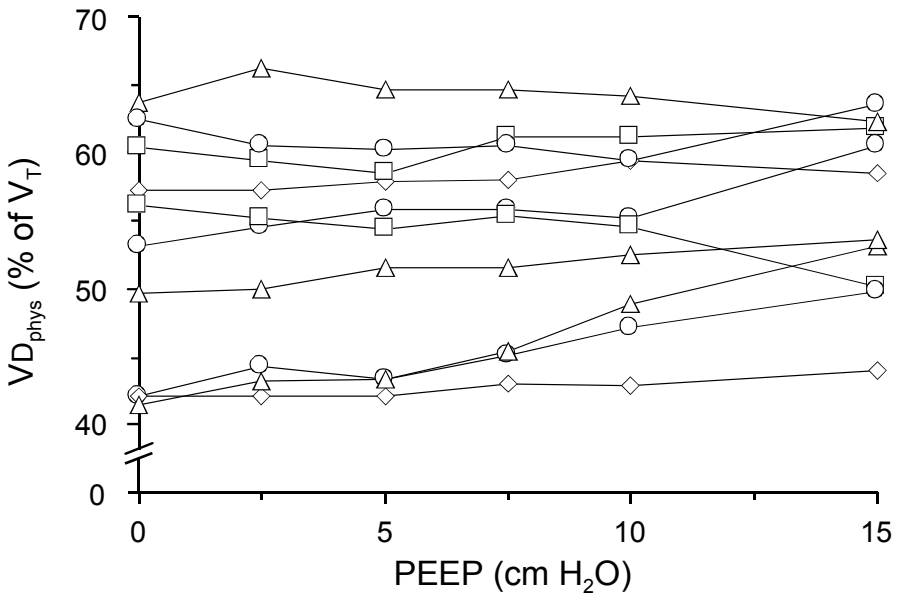


Figure 5. Modified from paper II. Physiological dead space ($V_{D_{phys}}$) at different positive end-expiratory pressure (PEEP) levels in each subject.

Total airway V_D ($V_{D_{Daw,tot}} = V_{D_{Daw,prox}} + V_{D_{Daw,dist}}$) increased slightly with PEEP while $V_{D_{alv}}$ did not change. However, individual differences were important: In patients with a positive response in PaO₂ with PEEP, the reduction in $V_{D_{alv}}$ compensated for the concurrent increase in $V_{D_{Daw,tot}}$. In negative PEEP responders, both $V_{D_{Daw,tot}}$ and $V_{D_{alv}}$ increased. Effects on V_D partitions may be important to study in attempts to reduce V_T and airway pressure.

\dot{V}_{CO_2} is affected by factors that alter gas distribution and diffusion. One such factor is time, defined as MDT [III]. \dot{V}_{CO_2} was overestimated by simulation at high RR and low V_T [I]. This can be explained by a decrease in MDT. In healthy pigs [III], $V_{Daw,dist}$ decreased from 29 to 22% as MDT increased from 0.51 to 1.39 s (apparatus V_D subtracted). Over the same MDT range, $V_{CO_2,T}$ increased by 10%. The effect of a longer MDT on $V_{Daw,dist}$ and $V_{CO_2,T}$ indicates a movement in the proximal direction of the “distal boundary of dead space” (72).

Healthy pigs have no collateral ventilation (73). Furthermore, different lung units probably fill and empty nearly synchronously. Obviously, the results cannot be applied on humans in whom collateral ventilation may equilibrate ventilation non-homogeneity. In addition, pendelluft may during a prolonged pause be important for ventilation equilibration in patients with obstructive lung disease. In any case, MDT affects gas exchange to such an extent that it may be of importance for optimisation of ventilator setting in ALI/ARDS. Studies of how variation of MDT affects \dot{V}_{CO_2} are needed in human subjects in health and in disease. Variation of post-inspiratory pause time and different inspiratory flow waveforms merit to be analysed in such studies. If effects of varying MDT differ considerably between individuals one would need to take the individual relationship between MDT and gas exchange into account. By studying a sequence of breaths with different MDT, this individual relationship may be easily defined, in order to complement the physiological profile.

In all papers traditional analytical principles were applied for parameterisation of lung properties. In the future it may be interesting to try alternative principles, for example artificial neural network (74).

In this thesis [I, IV] it was shown that simulation allows prediction of mechanics and gas exchange after resetting of the ventilator. A following step in the direction of Goal-Oriented Ventilation is to present the goals for the computer. Starting out from the physiological profile, the goals and limits of ventilator setting, the computer may search for an optimal setting leading to the goals. In principle, such a process is easily performed using iterative

simulation of different combinations of ventilator setting. Efficient search strategies must, however, be developed. In an ongoing study of optimisation of mechanical ventilation in experimental ARDS Goal-Oriented Ventilation in its full sense is being evaluated.

5.3 Concluding remarks

Simulation may be a tool in future Goal-Oriented Ventilation strategies. Simulation is easily done at the bedside. For determination of the physiological profile, upon which simulation is based, no complex or potentially dangerous procedures are needed. The physiological profile might need refinement with respect to non-linear elastic properties and the effect of mean distribution time on dead space. Simulation should be tested in wide groups of patients and in conjunction with clinically relevant types of resetting.

A large dead space has recently been associated with an increased risk of death in ARDS (75). A comprehensive analysis of lung function, particularly with regards to dead space, may offer valuable information of the patient's status, prognosis and response to treatment.

The conceptual development, presented in this thesis, will hopefully pave a way for better understanding of the complex physiology in critical lung disease and for optimisation of ventilator settings during mechanical ventilation.

6. Acknowledgements

A few years ago I was a student at Lund Medical School. Professor Björn Jonson caught my interest when he introduced the class to Clinical Physiology. Soon afterwards we met to discuss topics for a summer research scholarship. Computer simulation of mechanical ventilation was one among the diverse research projects that Björn presented to me. Since then, simulation has engaged much of my time. I am very grateful for the opportunity Björn gave me to perform the studies behind this thesis. His enormous knowledge and patience has been most encouraging.

I want to express my warmest gratitude to colleagues and friends for their help and advice. I thank Björn Drefeldt for programming and valuable discussions, Gerth-Inge Jönsson for constructing mechanical devices, Lisbet Niklason for programming and checking algorithms, Kerstin Brauer for help with figures and manuscripts, and Märta Granbohm for always being at hand with secretarial assistance. I thank Ingegerd Göransson, Elisabet Åström, Berit Olsson and Valéria Perez de Sa for valuable assistance during experiments. I thank Peter Lee Dahm for help with equipment and clinical insight.

Last, but not least, I thank my wife Magdalena for support and patience.

Financial support

This work was supported by grants from the Swedish Research Council (No 02872), the Swedish Heart Lung Foundation and the Medical Faculty of Lund University, Sweden.

The Servo Ventilators were supplied by Siemens-Elema AB, Solna, Sweden.

7. Sammanfattning

Respiratorbehandling är nödvändig då en patient på grund av kronisk eller akut lungsjukdom inte själv kan upprätthålla ett adekvat gasutbyte. Bakomliggande orsaker kan vara kronisk obstruktiv lungsjukdom, lunginflammation, blodförgiftning eller trauma. Respiratorbehandling kan i sig orsaka ytterligare skador på redan sjuka eller skadade lungor. Bland de faktorer som har identifierats som farliga finns högt luftvägstryck och övertänjning av lungvävnad. I åtskilliga studier har man undersökt strategier för att minska risken att tillfoga patienter lungskada. Det har exempelvis utmynnat i att låg andetagsvolym nu anses vara en av de viktigaste beståndsdelarna i ett lungskyddande ventilationsmönster. Det finns emellertid så många kombinationer av respiratorinställningar att det är omöjligt att resonera sig fram till en optimal inställning.

Det övergripande målet med denna avhandling var att utveckla och utvärdera en metod för datorsimulering av respiratorbehandling baserad på den enskilde patientens fysiologi. För att nå detta mål krävdes utveckling av metoder för analys av lungfunktion samt fördjupade kunskaper om hur en omställning av respiratorn påverkar gasutbytet.

Det kunde bekräftas att datorsimulering gör det möjligt att förutspå hur omställningar av viktiga respiratorparametrar påverkar luftvägstryck och gasutbyte. Den omfattande analys av lungfunktionen som presenteras kan ge viktig information om patientens komplexa fysiologi vid kritisk lungsjukdom, prognos och svar på behandling. Resultaten anger vägar för fortsatt utveckling av ett system för ”målorienterad respiratorinställning”. Denna princip innebär att läkaren anger vilka mål som skall uppnås med behandlingen. Datorn ger beslutsstöd genom att beräkna hur respiratorn skall ställas in för att nå målen.

8. References

1. Petersen GW, Baier H. Incidence of pulmonary barotrauma in a medical ICU. *Crit Care Med*. 1983;11:67–69.
2. Bouhuys A. Physiology and musical instruments. *Nature*. 1969;221:1199–1204.
3. Dreyfuss D, Saumon G. Barotrauma is volutrauma, but which volume is the one responsible? *Intensive Care Med*. 1992;18:139–141.
4. Slutsky AS. Lung injury caused by mechanical ventilation. *Chest*. 1999;116:9S–15S.
5. Taskar V, John J, Evander E, Wollmer P, Robertson B, Jonson B. Healthy lungs tolerate repetitive collapse and reopening during short periods of mechanical ventilation. *Acta Anaesthesiol Scand*. 1995;39:370–376.
6. Taskar V, John J, Evander E, Robertson B, Jonson B. Surfactant dysfunction makes lungs vulnerable to repetitive collapse and reexpansion. *Am J Respir Crit Care Med*. 1997;155:313–320.
7. Mead J, Takishima T, Leith D. Stress distribution in lungs: a model of pulmonary elasticity. *J Appl Physiol*. 1970;28:596–608.
8. Jonson B. Positive airway pressure: some physical and biological effects. In: Prakash O (ed). *Applied physiology in clinical respiratory care*. The Hague: Martinus Nihoff Publishers. 1982; pp. 125–139.
9. Tremblay LN, Slutsky AS. Ventilator-induced injury: from barotrauma to biotrauma. *Proc Assoc Am Physicians*. 1998;110:482–488.
10. Barber RE, Hamilton WK. Oxygen toxicity in man. A prospective study in patients with irreversible brain damage. *N Engl J Med*. 1970;283:1478–484.
11. Capellier G, Beuret P, Clement G, Depardieu F, Ract C, Regnard J, Robert D, Barale F. Oxygen tolerance in patients with acute respiratory failure. *Intensive Care Med*. 1998;24:422–428.
12. Cheng KC, Zhang H, Lin CY, Slutsky AS. Ventilation with negative airway pressure induces a cytokine response in isolated mouse lung. *Anesth Analg*. 2002;94:1577–1582.
13. Evander E, Wollmer P, Jonson B, Lachmann B. Pulmonary clearance of inhaled 99mTc-DTPA: effects of surfactant depletion by lung lavage. *J Appl Physiol*. 1987;62:1611–1614.

14. Evander E, Wollmer P, Jonson B. Pulmonary clearance of inhaled ^{99m}Tc-DTPA: effect of the detergent dioctyl sodium sulfosuccinate in aerosol. *Clin Physiol*. 1988;8:105–111.
15. John J, Taskar V, Evander E, Wollmer P, Jonson B. Additive nature of distension and surfactant perturbation on alveolocapillary permeability. *Eur Respir J*. 1997;10:192–199.
16. Liu JM, Evander E, Zhao J, Wollmer P, Jonson B. Alveolar albumin leakage during large tidal volume ventilation and surfactant dysfunction. *Clin Physiol*. 2001;21:421–427.
17. Seeger W, Stohr G, Wolf HR, Neuhofer H. Alteration of surfactant function due to protein leakage: special interaction with fibrin monomer. *J Appl Physiol*. 1985;58:326–338.
18. Lachmann B, Eijking EP, So KL, Gommers D. In vivo evaluation of the inhibitory capacity of human plasma on exogenous surfactant function. *Intensive Care Med*. 1994;20:6–11.
19. Ashbaugh DG, Bigelow DB, Petty TL, Levine BE. Acute respiratory distress in adults. *Lancet*. 1967;2:319–323.
20. Reynolds EO. Effect of alterations in mechanical ventilator settings on pulmonary gas exchange in hyaline membrane disease. *Arch Dis Child*. 1971;46:152–159.
21. Amato MB, Barbas CS, Medeiros DM, Magaldi RB, Schettino GP, Lorenzi-Filho G, Kairalla RA, Deheinzelin D, Munoz C, Oliveira R, Takagaki TY, Carvalho CR. Effect of a protective-ventilation strategy on mortality in the acute respiratory distress syndrome. *N Engl J Med*. 1998;338:347–354.
22. Ranieri VM, Suter PM, Tortorella C, De Tullio R, Dayer JM, Brienza A, Bruno F, Slutsky AS. Effect of mechanical ventilation on inflammatory mediators in patients with acute respiratory distress syndrome: a randomized controlled trial. *JAMA*. 1999;282:54–61.
23. ARDSnetwork. Ventilation with lower tidal volumes as compared with traditional tidal volumes for acute lung injury and the acute respiratory distress syndrome. *N Engl J Med*. 2000;342:1301–1308.
24. Brochard L, Roudot-Thoraval F, Roupie E, Delclaux C, Chastre J, Fernandez-Mondejar E, Clementi E, Mancebo J, Factor P, Matamis D, Ranieri M, Blanch L, Rodi G, Mentec H, Dreyfuss D, Ferrer M, Brun-Buisson C, Tobin M, Lemaire F. Tidal volume reduction for prevention of ventilator-induced lung injury in acute respiratory distress syndrome. The Multicenter Trial Group on Tidal Volume reduction in ARDS. *Am J Respir Crit Care Med*. 1998;158:1831–1838.

25. Stewart TE, Meade MO, Cook DJ, Granton JT, Hodder RV, Lapinsky SE, Mazer CD, McLean RF, Rogovein TS, Schouten BD, Todd TR, Slutsky AS. Evaluation of a ventilation strategy to prevent barotrauma in patients at high risk for acute respiratory distress syndrome. Pressure- and Volume-Limited Ventilation Strategy Group. *N Engl J Med*. 1998;338:355–361.
26. Brower RG, Shanholtz CB, Fessler HE, Shade DM, White P, Jr., Wiener CM, Teeter JG, Dodd-o JM, Almog Y, Piantadosi S. Prospective, randomized, controlled clinical trial comparing traditional versus reduced tidal volume ventilation in acute respiratory distress syndrome patients. *Crit Care Med*. 1999;27:1492–1498.
27. Eichacker PQ, Gerstenberger E, Banks SM, Cui X, Natanson C. A metaanalysis of ALI and ARDS trials testing low tidal volumes. In Press. *Am J Respir Crit Care Med*. 2002.
28. International consensus conferences in intensive care medicine: Ventilator-associated Lung Injury in ARDS. This official conference report was cosponsored by the American Thoracic Society, The European Society of Intensive Care Medicine, and The Societe de Reanimation de Langue Francaise, and was approved by the ATS Board of Directors, July 1999. *Am J Respir Crit Care Med*. 1999;160:2118–2124.
29. Laffey JG, Kavanagh BP. Carbon dioxide and the critically ill – too little of a good thing? *Lancet*. 1999;354:1283–1286.
30. Kavanagh B. Normocapnia vs hypercapnia. *Minerva Anesthesiol*. 2002;68:346–350.
31. Kregenow DA, Swenson ER. The lung and carbon dioxide: implications for permissive and therapeutic hypercapnia. *Eur Respir J*. 2002;20:6–11.
32. Pfeiffer B, Hachenberg T, Wendt M, Marshall B. Mechanical ventilation with permissive hypercapnia increases intrapulmonary shunt in septic and nonseptic patients with acute respiratory distress syndrome. *Crit Care Med*. 2002;30:285–289.
33. Feihl F, Eckert P, Brimiouille S, Jacobs O, Schaller MD, Melot C, Naeije R. Permissive hypercapnia impairs pulmonary gas exchange in the acute respiratory distress syndrome. *Am J Respir Crit Care Med*. 2000;162:209–215.
34. Kolobow T, Gattinoni L, Tomlinson TA, Pierce JE. Control of breathing using an extracorporeal membrane lung. *Anesthesiology*. 1977;46:138–141.

35. Jonzon A, Öberg PA, Sedin G, Sjöstrand U. High frequency low tidal volume positive pressure ventilation. *Acta Physiol Scand*. 1970;80:21A-22A.
36. Heijman K, Heijman L, Jonzon A, Sedin G, Sjöstrand U, Widman B. High frequency positive pressure ventilation during anaesthesia and routine surgery in man. *Acta Anaesthesiol Scand*. 1972;16:176-187.
37. Lunkenheimer PP, Frank I, Ising H, Keller H, Dickhut HH. Intrapulmonaler Gaswechsel unter simulierter Apnoe durch transtrachealen periodischen intrathorakalen Druckwechsel. *Anaesthesist*. 1973;22:232-238.
38. Hamilton PP, Onayemi A, Smyth JA, Gillan JE, Cutz E, Froese AB, Bryan AC. Comparison of conventional and high-frequency ventilation: oxygenation and lung pathology. *J Appl Physiol*. 1983;55:131-138.
39. Dorrington KL, McRae KM, Gardaz JP, Dunnill MS, Sykes MK, Wilkinson AR. A randomized comparison of total extracorporeal CO₂ removal with conventional mechanical ventilation in experimental hyaline membrane disease. *Intensive Care Med*. 1989;15:184-191.
40. Niblett DJ, Sandhar BK, Dunnill MS, Sykes MK. Comparison of the effects of high frequency oscillation and controlled mechanical ventilation on hyaline membrane formation in a rabbit model of the neonatal respiratory distress syndrome. *Br J Anaesth*. 1989;62:628-636.
41. Jonson B, Lachmann B. Setting and monitoring of high-frequency jet ventilation in severe respiratory distress syndrome. *Crit Care Med*. 1989;17:1020-1024.
42. Gerstmann DR, Minton SD, Stoddard RA, Meredith KS, Monaco F, Bertrand JM, Battisti O, Langhendries JP, Francois A, Clark RH. The Provo multicenter early high-frequency oscillatory ventilation trial: improved pulmonary and clinical outcome in respiratory distress syndrome. *Pediatrics*. 1996;98:1044-1057.
43. Gerstmann DR, Wood K, Miller A, Steffen M, Ogden B, Stoddard RA, Minton SD. Childhood outcome after early high-frequency oscillatory ventilation for neonatal respiratory distress syndrome. *Pediatrics*. 2001;108:617-623.
44. MacIntyre NR. High-frequency jet ventilation. *Respir Care Clin N Am*. 2001;7:599-610.

45. Jonson B, Lachmann B, Fletcher R. Monitoring of physiological parameters during high frequency ventilation (HFV). *Acta Anaesthesiol Scand Suppl.* 1989;90:165–169.
46. Bryan AC, Cox PN. History of high frequency oscillation. *Schweiz Med Wochenschr.* 1999;129:1613–1616.
47. Richecoeur J, Lu Q, Vieira SR, Puybasset L, Kalfon P, Coriat P, Rouby JJ. Expiratory washout versus optimization of mechanical ventilation during permissive hypercapnia in patients with severe acute respiratory distress syndrome. *Am J Respir Crit Care Med.* 1999;160:77–85.
48. Jonson B, Similowski T, Levy P, Viires N, Pariente R. Expiratory flushing of airways: a method to reduce deadspace ventilation. *Eur Respir J.* 1990;3:1202–1205.
49. De Robertis E, Sigurdsson SE, Drefeldt B, Jonson B. Aspiration of airway dead space. A new method to enhance CO₂ elimination. *Am J Respir Crit Care Med.* 1999;159:728–732.
50. Dreyfuss D, Saumon G. Evidence-based medicine or fuzzy logic: what is best for ARDS management? *Intensive Care Med.* 2002;28:230–234.
51. Suter PM, Fairley B, Isenberg MD. Optimum end-expiratory airway pressure in patients with acute pulmonary failure. *N Engl J Med.* 1975;292:284–289.
52. Hedenstierna G. The effect of respiratory frequency on pulmonary function during artificial ventilation. A review. *Acta Anaesthesiol Scand.* 1976;20:20–31.
53. Mercat A, Diehl JL, Michard F, Anguel N, Teboul JL, Labrousse J, Richard C. Extending inspiratory time in acute respiratory distress syndrome. *Crit Care Med.* 2001;29:40–44.
54. Rippe B, Levin L. Computer simulations of ultrafiltration profiles for an icodextrin-based peritoneal fluid in CAPD. *Kidney Int.* 2000;57:2546–2556.
55. Jansson L, Jonson B. A theoretical study on flow patterns of ventilators. *Scand J Respir Dis.* 1972;53:237–246.
56. Fletcher R, Werner O, Nordström L, Jonson B. Sources of error and their correction in the measurement of carbon dioxide elimination using the Siemens-Elema CO₂ Analyzer. *Br J Anaesth.* 1983;55:177–185.

57. Rohrer F. Der Strömungswiderstand in den menschlichen Atemwegen und der Einfluss der unregelmässigen Verzweigung des Bronchialsystems auf den Atmungsverlauf. *Archiv für die gesamte Physiologie*. 1915;162:225–299.
58. Liu JM, De Robertis E, Blomquist S, Dahm PL, Svantesson C, Jonson B. Elastic pressure-volume curves of the respiratory system reveal a high tendency to lung collapse in young pigs. *Intensive Care Med*. 1999;25:1140–1146.
59. Svantesson C, John J, Taskar V, Evander E, Jonson B. Respiratory mechanics in rabbits ventilated with different tidal volumes. *Respir Physiol*. 1996;106:307–316.
60. Briscoe WA, Dubois AB. The relationship between airway resistance, airway conductance and lung volume in subjects of different age and body size. *J Clin Invest*. 1958;37:1279–1285.
61. Fletcher R, Jonson B, Cumming G, Brew J. The concept of dead space with special reference to the single breath test for carbon dioxide. *Br J Anaesth*. 1981;53:77–88.
62. Wolff G, Brunner JX. Series dead space volume assessed as the mean value of a distribution function. *Int J Clin Monit Comput*. 1984;1:177–181.
63. Åström E, Niklason L, Drefeldt B, Bajc M, Jonson B. Partitioning of dead space – a method and reference values in the awake human. *Eur Respir J*. 2000;16:659–664.
64. Wolff G, Brunner J, Weibel W, Bowes C, Muchenberger R, Bertschmann W. Anatomical serial dead space volume; concept and measurement in clinical praxis. *Applied Cardiopulmonary Pathology*. 1989;2:299–307.
65. Eriksson L, Wollmer P, Olsson CG, Albrechtsson U, Larusdottir H, Nilsson R, Sjögren A, Jonson B. Diagnosis of pulmonary embolism based upon alveolar dead space analysis. *Chest*. 1989;96:357–362.
66. Jonson B, Beydon L, Brauer K, Månsson C, Valind S, Grytzell H. Mechanics of respiratory system in healthy anesthetized humans with emphasis on viscoelastic properties. *J Appl Physiol*. 1993;75:132–140.
67. Beydon L, Svantesson C, Brauer K, Lemaire F, Jonson B. Respiratory mechanics in patients ventilated for critical lung disease. *Eur Respir J*. 1996;9:262–273.

68. Ranieri VM, Zhang H, Mascia L, Aubin M, Lin CY, Mullen JB, Grasso S, Binnie M, Volgyesi GA, Eng P, Slutsky AS. Pressure-time curve predicts minimally injurious ventilatory strategy in an isolated rat lung model. *Anesthesiology*. 2000;93:1320–1328.
69. Gottfried SB, Rossi A, Calverley PM, Zocchi L, Milic-Emili J. Interrupter technique for measurement of respiratory mechanics in anesthetized cats. *J Appl Physiol*. 1984;56:681–690.
70. Similowski T, Levy P, Corbeil C, Albala M, Pariente R, Derenne JP, Bates JH, Jonson B, Milic-Emili J. Viscoelastic behavior of lung and chest wall in dogs determined by flow interruption. *J Appl Physiol*. 1989;67:2219–2229.
71. Eissa NT, Ranieri VM, Corbeil C, Chasse M, Braidy J, Milic-Emili J. Effects of positive end-expiratory pressure, lung volume, and inspiratory flow on interrupter resistance in patients with adult respiratory distress syndrome. *Am Rev Respir Dis*. 1991;144:538–543.
72. Bowes CL, Richardson JD, Cumming G, Horsfield K. Effect of breathing pattern on gas mixing in a model with asymmetrical alveolar ducts. *J Appl Physiol*. 1985;58:18–26.
73. Woolcock AJ, Macklem PT. Mechanical factors influencing collateral ventilation in human, dog, and pig lungs. *J Appl Physiol*. 1971;30:99–115.
74. Perchiizzi G, Högman M, Rylander C, Giuliani R, Fiore T, Hedenstierna G. Assessment of respiratory system mechanics by artificial neural networks: an exploratory study. *J Appl Physiol*. 2001;90:1817–1824.
75. Nuckton TJ, Alonso JA, Kallet RH, Daniel BM, Pittet JF, Eisner MD, Matthay MA. Pulmonary dead-space fraction as a risk factor for death in the acute respiratory distress syndrome. *N Engl J Med*. 2002;346:1281–1286.

Appendix
Papers I – IV

Errata

Paper I

Unfortunately, the publisher did not make the corrections indicated in the author's galley proof before printing. In this reproduction the following errors in the original article have been corrected:

	Original article	Corrected
Page 292, equation 7	Double integral	Single integral
Page 292, equation 9	$P_{\text{vent,E}}$	P_{vent}
Page 292, results	$0.94 \text{ ml}\cdot\text{min}\cdot\text{kg}^{-1}$	$0.94 \text{ ml}\cdot\text{min}^{-1}\cdot\text{kg}^{-1}$
Table 1, unit column	$V_{\text{CO}_2,\text{E}}$, mL CO	$V_{\text{CO}_2,\text{E}}$, mL CO ₂
Table 1, unit column	R_{I} , cm H ₂ O ·s·L ⁻¹	R_{I} , cm H ₂ O ·s·L ⁻¹
Table 1, for all individual and average values of V_{Daw} and C a decimal were erroneously printed	Example: V_{Daw} for pig 1 6.1	61
Page 294, figure legend 5	(())	(<>)

Paper II

In this reproduction the following errors in the original article have been corrected:

Table 1, Lung Injury Score, subject 4	1.50	1.75
Page 1243, last paragraph	14%	9%

Computer-aided ventilator resetting is feasible on the basis of a physiological profile

L UTTMAN and B JONSON

Department of Clinical Physiology, University Hospital, Lund, Sweden, Supported by the Swedish Medical Research Council(02872) and the Swedish Heart Lung Foundation

Background: Ventilator resetting is frequently needed to adjust tidal volume, pressure and gas exchange. The system comprising lungs and ventilator is so complex that a trial and error strategy is often applied. Comprehensive characterization of lung physiology is feasible by monitoring. The hypothesis that the effect of ventilator resetting could be predicted by computer simulation based on a physiological profile was tested in healthy pigs.

Methods: Flow, pressure and CO₂ signals were recorded in 7 ventilated pigs. Elastic recoil pressure was measured at post-inspiratory and post-expiratory pauses. Inspiratory and expiratory resistance as a function of volume and compliance were calculated. CO₂ elimination per breath was expressed as a function of tidal volume. Calculating pressure and flow moment by moment simulated the effect of ventilator action, when respiratory rate was varied between 10 and 30 min⁻¹ and minute vol-

ume was changed so as to maintain PaCO₂. Predicted values of peak airway pressure, plateau pressure, and CO₂ elimination were compared to values measured after resetting.

Results: With 95% confidence, predicted pressures and CO₂ elimination deviated from measured values with < 1 cm H₂O and < 6%, respectively.

Conclusion: It is feasible to predict effects of ventilator resetting on the basis of a physiological profile at least in health.

Received 10 April 2001, accepted for publication 20 August 2001

Keywords: dead space, gas exchange, mechanics, pulmonary, swine

© Acta Anaesthesiologica Scandinavica 46 (2002)

CONTROLLED mechanical ventilation is frequently used in patients with critical lung disease such as acute lung injury and sometimes in acute respiratory insufficiency in chronic obstructive pulmonary disease. These groups are characterized by a very complex pathophysiology. Since the early 70s the optimal mode of mechanical ventilation in various critical lung diseases is a debated issue. For example, Reynolds treated infants with respiratory distress syndrome with pressure limited ventilation and inverse I:E ratio (1). An early study based upon mathematical simulation of various patterns of ventilation indicated that an optimal pattern depends on the patient's pathophysiology (2). During mechanical ventilation, modern monitoring technique allows automated analysis of both mechanics and CO₂ elimination, so as to illustrate the pathophysiology of the patient. The task of the physician or therapist is to combine this physiological profile with all available clinical information and on this basis decide about the mode of ventilation and exact ventilator setting. The physiological profile and all possible setting variations combine to an overwhelmingly complex system. In the

clinic, ventilators are not seldom reset on a trial and error basis. The result, particularly with respect to PaCO₂, cannot be judged until after 15–30 min (3). During that period a change of basic status of the patient may obscure the effect of resetting. Such strategies appear inefficient. An alternative strategy is to let the computer simulate an intended change of ventilator setting on the basis of information provided by the physiological profile. From the result of the simulation the physician could beforehand judge if the intentions should be carried through or if alternative settings should be analyzed. A prerequisite for the simulation would be that relevant physiological properties are expressed in mathematical terms.

The change in CO₂ elimination per minute (VCO₂) occurring after a change in alveolar ventilation will indicate the change in PaCO₂ at a new steady state (3). VCO₂ after resetting was therefore used as an index of changing CO₂ equilibrium.

This study should be regarded as an initial step in the development of systems for computer-aided ventilator resetting. One objective of the present study was to develop a technique for measurements based

upon a simple lung model. The main objective was to test the hypothesis that mechanical behavior and V_{CO_2} after resetting the ventilator could be predicted by simulation in healthy pigs. The study also complements the knowledge about lung physiology in anesthetized paralyzed pigs.

Methods

The local Ethics Board of Animal Research approved the experimental protocol. Seven pigs of the Swedish landrace, average weight 30.8 kg (27.1–33.5), were fasted overnight with free access to water. The animals were premedicated with azaperon (Stresnil®, Jansen, Beerse, Belgium), 7 mg/kg, anesthetized with ketamin (Ketalar®, Parke-Davis, Morris Plains, USA), 5 mg/kg, into an ear vein, intubated with a 7.0-mm ID tracheal tube, and connected to a ventilator (Servo Ventilator 900C, Siemens-Eléma, Solna, Sweden). The ventilator produced a square inspiratory flow pattern at a baseline setting of respiratory rate (RR) 20 min^{-1} , inspiratory time (TI) 33%, postinspiratory pause time 10% and a positive end-expiratory pressure set on the ventilator (PEEP) of 6 cm H_2O . The fraction of inspired oxygen was 0.21. The baseline minute ventilation (MV) was adjusted to achieve a $PaCO_2$ of 4.5–5.0 kPa. A mainstream analyzer (CO_2 Analyzer 930, Siemens-Eléma, Solna, Sweden) measured concentration of CO_2 in expired and inspired gas (C_{CO_2}). Anesthesia was maintained by continuous infusion of ketamin, 17 mg/kg/h, midazolam (Dormicum®, Hoffmann-La Roche AG, Basel, Switzerland), 1.7 mg/kg/h and pancuronium bromide (Pavulon®, Organon Teknika, Bostel, Holland), 0.5 mg/kg/h. The ventilator/computer system used for data recording has previously been described (4). Signals from the ventilator and CO_2 analyzer representing flow rate, pressure in the expiratory line of the ventilator (P_{vent}) and C_{CO_2} were sampled by a personal computer at the frequency of 50 Hz. Flow, pressure and CO_2 signals had a 50% response time of 12 ms and were synchronous within ± 8 ms (5). There were no dropouts among the animals.

Protocol

After preparation of the pigs a recruitment maneuver was performed by inflating the lungs with a pressure of 35 cm H_2O for 10 s to standardize conditions among the animals by reducing airway closure and atelectasis induced during the induction of anesthesia (6). The system was tested for leakage. A study sequence comprised 10 normal breaths, one breath with a post-inspiratory pause, another four normal breaths and

one with a post-expiratory pause. The recording continued during ventilator resetting and two minutes thereafter.

The experimental protocol was designed to allow five settings to be studied during a short period at a physiological steady state. After a perturbation of CO_2 equilibrium extended periods are needed to restore a steady state (3). Perturbation of CO_2 equilibrium was avoided by increasing MV at higher RR in order to compensate for the higher physiological dead space fraction associated with reduced tidal volume (V_T). In order to keep V_{CO_2} constant we performed in each pig a an initial study sequence to examine how CO_2 elimination per breath ($V_{CO_2,T}$) varied in relation to V_T , as further described below.

Then, alternative settings were studied. These were changes in RR from 20 to 10, 15, 25 and 30 coupled to estimated changes in MV in randomized order. Recorded data immediately before each resetting were used to establish the physiological profile serving as basis for simulation of the ensuing setting. Recorded data starting 30s after resetting, covering 10 breaths were used to measure peak airway pressure (P_{peak}), postinspiratory quasi-static elastic recoil pressure ($P_{plateau}$) and V_{CO_2} which were compared to simulated data.

Data analysis

Data sampled during a study sequence were transferred to a spreadsheet (Microsoft® Excel 97, Microsoft Corp., Readmond, WA) for analysis. Flow measured in the inspiratory and expiratory circuits within the ventilator included flow that did not reach the animal. In order to obtain airway flow rate (V'_{aw}), measured flow rate was corrected for the compliance in the tubings by subtraction from each flow sample the product between compliance and rate of pressure change (7). The expiratory flow signal was normalized so that, at steady state, expired V_T equaled inspired V_T (7). Volume relative to end-expiratory volume (V) was calculated by integration of V'_{aw} .

A lung model was defined prior to data analysis. As a goal was to develop methods, which can be applied in the clinic, the model should only incorporate features, which can easily be studied with techniques available at the bedside. Accordingly, minimal interference with ordinary pattern of mechanical ventilation at the phase of parameter estimation to establish the physiological profile should yield sufficiently detailed information to allow proper simulation of alternative ventilator settings. As a result, a mono-compartment model without viscoelastic properties or inertia was employed. Furthermore, constant values

for compliance of the respiratory system (C) and inspiratory conductance (G_I) were applied on the basis of prior data (6, 8). Expiratory conductance (G_E) was assumed to vary as a linear function of volume (9). The resistance of the Y-piece, CO₂ transducer connector, tracheal tube, ventilator tubing and the expiratory line of the ventilator were considered flow dependent according to Rohrer (10). The coefficients defining resistance of the connecting system were determined *in vitro* by measuring flow rate and pressure at variable flow rate delivered from the ventilator through the connecting system into open air. Tube compliance was measured as the quotient between volume of gas 'expired' from the tubing after an 'inspiration', during which the tracheal tube was completely occluded, and the preceding $P_{plateau} \cdot V_{CO_2,T}$ and V_{CO_2} and their variation with V_T was determined from the single breath test for CO₂ (SBT-CO₂).

The following equations 1–9 were used for the establishment of the physiological profile and in the simulation process.

$P_{plateau}$ and post-expiratory quasi-static elastic recoil pressure ($P_{el,E}$) were read 0.3 s after flow cessation. This time corresponds to the duration of the postinspiratory pause at baseline ventilator setting. C was calculated as:

$$C = V_T / (P_{plateau} - P_{el,E}) \quad (1)$$

The pressure that drives flow through the tracheal tube (P_{tube}) was determined as a function of flow

$$P_{tube} = R_{tube} \cdot V'_{aw} = (k_0 + k_1 \cdot |V'_{aw}|) \cdot V'_{aw} \quad (2)$$

k_0 and k_1 describe tube resistance (R_{tube}) and its variation with flow due to turbulence. Tracheal pressure (P_{tr}) was calculated from measured P_{vent} and calculated P_{tube} :

$$P_{tr} = P_{vent} - P_{tube} \quad (3)$$

The pressure overcoming resistance of the respiratory system (P_{res}) was calculated as the difference between P_{tr} and the elastic recoil pressure, i.e. V/C :

$$P_{res} = P_{tr} - V/C \quad (4)$$

G_I and G_E were calculated as V'_{aw}/P_{res} . For each respiratory phase a linear regression of conductance over the volume range from 15 to 85% of V_T was made, thus avoiding the influence from fast accelerations and decelerations at flow transitions. As G_I does not vary significantly during the V_T a constant value for G_I was calculated from the regression at mid-inspiration. G_E may according to previous studies be described as a linear function of volume (9). Accordingly:

$$G_E = g_0 + g_1 \cdot V \quad (5)$$

g_0 denotes conductance at zero volume and g_1 gives variation of G_E and its reciprocal expiratory resistance (R_E) with volume.

$V_{CO_2,T}$ reflects the difference between volume of CO₂ expired ($V_{CO_2,E}$) and the volume of CO₂ re-inspired at the start of inspiration ($V_{CO_2,I}$) (Fig.1). $V_{CO_2,T}$ at current ventilation was calculated by integration of C_{CO_2} by volume over the respiratory cycle. To determine how $V_{CO_2,T}$ would vary in response to variations in V_T the SBT-CO₂ was further analyzed. The alveolar plateau of the CO₂ concentration during expiration ($C_{CO_2,A}$) was approximated according to .6 applied over the last 40% of the volume expired (VE):

$$C_{CO_2,A}(V_E) = f_0 + f_1 \cdot \ln(V_E) \quad (6)$$

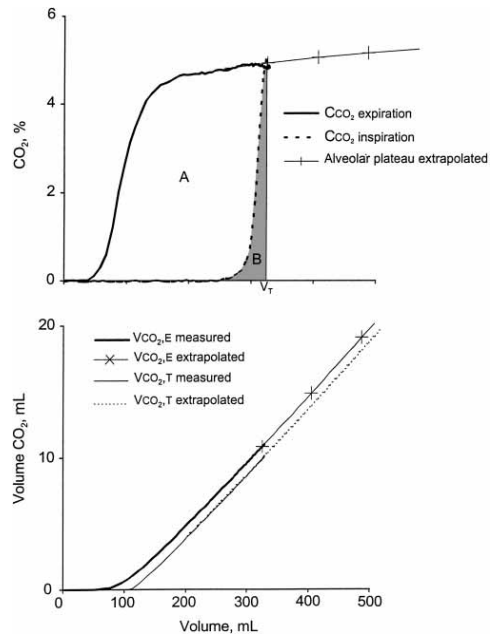


Fig.1. Upper panel: The single breath test for CO₂ shows expiratory CO₂ (heavy line) and inspiratory CO₂ (interrupted line) together delineating area A that corresponds to CO₂ elimination per breath ($V_{CO_2,T}$). Area B represents volume of CO₂ re-inspired from the Y-piece and ventilator tubing ($V_{CO_2,I}$). For calculation of how expired volume of CO₂ (area A + B, i.e. $V_{CO_2,E}$) varies with tidal volume (V_T) the alveolar plateau was described mathematically and extrapolated (crossed line, .6). Lower panel: The heavy and crossed lines represent integration of the information in upper panel (.7) yielding $V_{CO_2,E}$ as a function of volume. Thin and dotted lines represent $V_{CO_2,T}$ obtained by subtraction of $V_{CO_2,I}$ (.8) from $V_{CO_2,E}$.

The equation has been applied in previous studies (11, 12)

$V_{CO_2,E}$ at an alternative tidal volume ($V_{T,alt}$) was calculated:

$$V_{CO_2,E}(V_{T,alt}) = V_{CO_2,E}(V_T) + \int_{V_T}^{V_{T,alt}} C_{CO_2} \cdot A \cdot dV_E \quad (7)$$

The second term in . 7 is derived from . 6 as illustrated in Fig. 1.

$V_{CO_{2,I}}$ at $V_{T,alt}$ was approximated:

$$V_{CO_{2,I}}(V_{T,alt}) = \frac{V_{CO_{2,I}}(V_T) \cdot C_{CO_{2,ET}}(V_{T,alt})}{C_{CO_{2,ET}}(V_T)} \quad (8)$$

$C_{CO_{2,ET}}$ is the end-tidal C_{CO_2} .

The parameters ($V_{CO_2,E}$, $V_{CO_2,I}$, $C_{CO_2,ET}$, f_0 , f_1 , C , G_I , g_0 and g_1) together with corresponding equations mathematically characterize lung function. These parameters represent the physiological profile of the subject.

Simulation of an alternative mode of ventilation

In the present study simulations of volume controlled ventilation were performed. The simulation process mimics this mode by keeping the simulated inspiratory flow rate constant and, during expiration, by not allowing P_{vent} to fall below PEEP. During early expiration P_{vent} is higher than PEEP. This prevails as long as ventilator resistance at fully open expiratory valve multiplied by expiratory flow is higher than PEEP.

Mathematical simulation of ventilator function was stepwise performed by dividing the respiratory cycle into short time intervals. During each interval the pressures in the Y-piece, trachea and alveoli, as well as flow rate and lung volume were calculated. The basic time interval used in the simulation was 1% of the breathing cycle so as to divide the breath into 100 intervals. In order to avoid oscillations at sudden pressure and flow changes the time interval during phase transitions was reduced to 0.001% of the cycle. For the same reason, filtering of the values for R_{tube} , P_{vent} and expiratory V'_{aw} was performed. The fraction 0.7 of the filtered value from the previous time interval was added to the value calculated for the current interval. This sum was divided by 1.7 in order not to change the magnitude of the parameters. The first time interval during expiration needed a special 'filter'. For that interval V'_{aw} was set to be 0.4 times a value of V'_{aw} calculated as described in . 9. The coefficients 0.7 and 0.4 were empirically found to allow simulation of various patterns of ventilation without severe artifacts related to system oscillation.

During inspiration V'_{aw} was determined by MV, RR and T_I . V was obtained as the integral of V'_{aw} . Elastic recoil pressure (P_{el}) and P_{tube} were calculated using . 1 and . 3. During expiration V'_{aw} was calculated as

$$V'_{aw} = (P_{el} - P_{vent}) / (R_E + R_{tube}) \quad (9)$$

The value of V was transferred from the previous interval. Other variable's values were calculated from the current interval. Six consecutive breaths were simulated. Simulated values of P_{peak} , $P_{plateau}$ and V_{CO_2} at the 6th simulated breath were compared to the average recorded values from 10 breaths starting 30 s after resetting. The spreadsheet used for simulations is available from the authors.

Statistical methods

The Student's paired two-tailed *t*-test was used to analyze differences between simulated values and measured values of P_{peak} , $P_{plateau}$ and V_{CO_2} . Wilcoxon matched pair signed rank sum test was used to determine whether the precision of P_{peak} and $P_{plateau}$ simulations made at RR 10, 15, 25 and 30 was significantly different from those made at baseline RR 20. A *P*-value of < 0.05 was considered significant.

Results

Baseline characteristics of the animals including the physiological profile are shown in Table 1. To reach the target end-tidal CO_2 at an RR of 20 min^{-1} a V_T of on average $9.4 \pm 0.95 \text{ ml} \cdot \text{kg}^{-1}$ was required. This relates to a CO_2 production of $5.7 \pm 0.94 \text{ ml} \cdot \text{min}^{-1} \cdot \text{kg}^{-1}$. The SBT- CO_2 showed a distinct increase of CCO_2 and a clearly delineated transition to the alveolar plateau (Fig. 1). The slope of the alveolar plateau at the end of V_T was in the range 0.09–0.26% per 100 ml. $V_{CO_{2,I}}$ was on average $8 \pm 1.3\%$ of $V_{CO_{2,E}}$.

Mid-tidal expiratory resistance ($R_{E,MID}$) was in each pig higher than inspiratory resistance (R_I). $R_{E,MID}$ correlated to R_I ($r^2 = 0.89$, $P < 0.01$) Fig. 2. Expiratory conductance decreased during expiration in 6 of 7 pigs, as indicated by a positive g_1 . The average resistance over the V_T is shown in Fig. 2. Compliance was $38 \pm 4.5 \text{ ml cm H}_2\text{O}^{-1}$.

In each case the simulation was in steady state already after 3 of the 6 simulated breaths as shown in a representative example (Fig. 3). Simulated P_{vent}/V , P_{tr}/V and P_{el}/V loops differed from loops calculated from measured flow and pressure, owing to simulation filtering (Fig. 4). The last simulated breath was compared to the average of 10 measured breaths before and after resetting. The difference was expressed as percent of the measured value (Fig. 5). The simula-

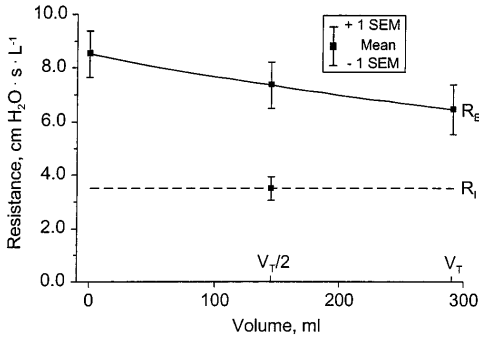


Fig. 2. Resistance. Illustration of the considered constant (6,7) inspiratory resistance (R_I) and the variable expiratory resistance (R_E) (. 5) as average and SEM of the 7 pigs.

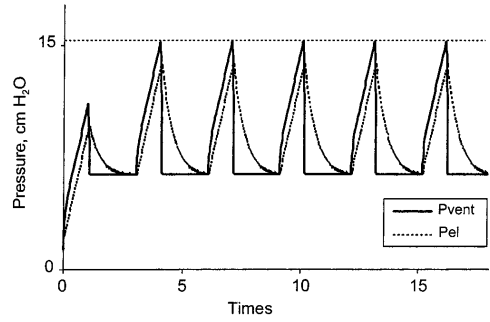


Fig. 3. Simulated pressure in the ventilator (P_{vent}) and elastic recoil pressure (P_{el}) illustrate that simulation reached a steady state after about 3 out of 6 breaths, as in this example.

tion of events before resetting, i.e. at RR 20, served as control of the process comprising measurements, modeling, parameterization and simulation. Then V_{CO_2} showed nearly identity between simulated and measured values. At RR 20, P_{peak} and $P_{plateau}$ showed differences below 4% in each case ($P > 0.05$). Simulation of V_{CO_2} after resetting of RR and V_T resulted in values which were not significantly different from measured values at reduced RR. However at RR 25 and particularly at RR 30 simulation resulted in an overestimation of V_{CO_2} ($P = 0.003$ and $P < 0.001$, respectively). After resetting measured ranges of P_{peak} and $P_{plateau}$ were 12–25 cm H_2O and 11–24 cm H_2O , respectively. Out of simulated values 95% differed less than 1.0 cm H_2O from measured values. Simulated $P_{plateau}$ was marginally higher than measured at RR 25 and RR 30 ($P < 0.001$, $P = 0.025$, respectively). The

precision of simulations of pressures after resetting, i.e. at RR 10, 15, 25 and 30, were not significantly different from those before resetting, at RR 20.

Discussion

The present results contribute to the knowledge about respiratory physiology in pigs. Compliance, on average 1.2 ml/kg, was similar to data previously reported (6). No comparable data on resistance of the respiratory system have been found. Expiratory resistance higher than inspiratory and increasing toward the end of expiration is known in humans (7). This reflects that the resistive pressure drop in the airways reduces transbronchial pressure during expiration while the opposite is true during inspiration (7). An error in the

Table 1

Baseline characteristics of the animals.

	Pig 1	Pig 2	Pig 3	Pig 4	Pig 5	Pig 6	Pig 7	Average	SD
Weight, kg	33.0	32.2	29.2	29.9	27.1	31.0	33.5	30.8	2.3
V_T , mL · kg ⁻¹	10.1	10.1	9.4	9.7	7.4	9.1	10.0	9.4	0.95
V_{CO_2} , mL · kg ⁻¹ · min ⁻¹	6.7	6.0	5.3	6.1	3.8	5.8	6.4	5.7	0.94
V_{Dawn} , mL	61	66	62	49	52	69	70	61	8.1
$V_{CO_2,i}$, mL CO ₂	0.9	0.8	0.8	0.8	0.6	0.8	0.9	0.8	0.09
$V_{CO_2,e}$, mL CO ₂	12.1	10.5	8.7	10.1	5.9	9.9	11.7	9.8	2.09
$C_{CO_2,A}$, % CO ₂	4.8	4.5	4.7	4.7	4.8	5.4	4.8	4.8	0.27
f_{iO_2} , % CO ₂	3.1	1.5	2.5	2.8	2.0	2.2	2.5	2.4	0.54
f_{iCO_2} , % CO ₂	0.3	0.5	0.4	0.3	0.5	0.6	0.4	0.4	0.11
Compliance, mL · cm H ₂ O ⁻¹	42	34	34	32	40	41	43	38	4.5
R_I , cm H ₂ O · s · L ⁻¹	2.1	3.9	3.1	4.7	3.2	5.2	2.3	3.5	1.1
$R_{E,MID}$, cm H ₂ O · s · L ⁻¹	6.1	9.9	7.9	10.4	5.7	10.8	5.7	8.1	2.3
g_0 , L · s ⁻¹ · cm H ₂ O ⁻¹	0.14	0.10	0.11	0.08	0.11	0.09	0.19	0.12	0.036
g_1 , s ⁻¹ · cm H ₂ O ⁻¹	$1.5 \cdot 10^{-4}$	$1.5 \cdot 10^{-5}$	$1.3 \cdot 10^{-4}$	$8.2 \cdot 10^{-5}$	$5.2 \cdot 10^{-4}$	$1.1 \cdot 10^{-5}$	$-2.0 \cdot 10^{-3}$	$1.3 \cdot 10^{-4}$	$7.8 \cdot 10^{-4}$

estimate of elastic recoil pressure at mid- V_T leading to an overestimation of R_I would lead to underestimation of $R_{E,MID}$, and vice versa. The close correlation between R_I and $R_{E,MID}$ suggests that the linear elastic pressure volume relationship based upon measured values before and after an inspiration is valid. The model of mechanical behavior, which was defined prior to the study, is supported by internal coherence of the observations and principle agreement with previous data. Airway deadspace corrected for tube deadspace (V_{Daw}), on average 2.0 ml/kg body weight, appears larger than data reported in humans (13). The clearly delineated, nearly flat alveolar plateau of the SBT- CO_2 signifies that among lung units, which empty in sequence, ventilation/perfusion ratio (V/Q) is nearly even in healthy pigs. The classical SBT- CO_2

was complemented by its inspiratory limb so as to create a loop. This allows measurement of re-inspired CO_2 resident in the circuit proximal to the site where CO_2 is measured. Re-inspiration of about 8% of the expired volume of CO_2 reflects a deadspace in the Y-piece and, because of turbulence, in the adjacent tubings (5). The model for CO_2 elimination incorporates features allowing for uneven V/Q leading to a sloping alveolar plateau, which probably is needed only in disease.

Previous authors have stressed that the physiological

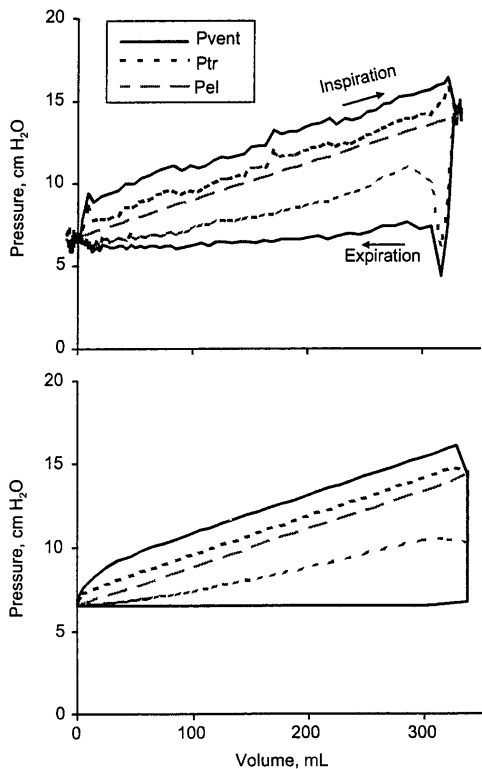


Fig. 4. Upper panel shows measured pressure in the ventilator (P_{vent}) during a breath and elastic recoil pressure (P_{el}) obtained by interpolation from data measured during pauses. Tracheal pressure (P_{tr}) was calculated from P_{vent} by subtraction (. 2-3). Lower panel illustrates the same pressures simulated.

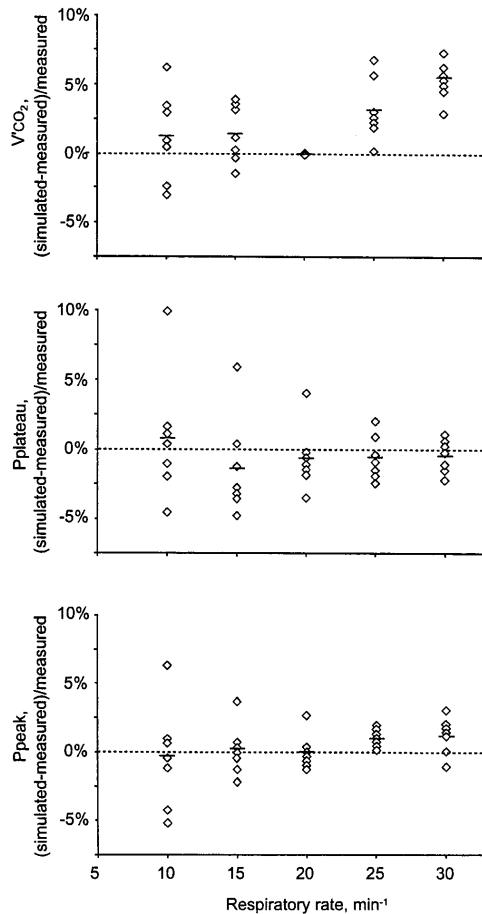


Fig. 5. Individual (\diamond) and average (—) errors in simulation of CO_2 elimination per minute (V_{CO_2}), postinspiratory quasi-static plateau pressure ($P_{plateau}$) and peak airway pressure (P_{peak}) at different respiratory rates. A positive value corresponds to an overestimation.

effects of ventilator resetting are difficult or impossible to predict because of the complexity of the total system comprising ventilator and lungs (14, 15). In principle, such predictions may be performed if the properties of the total system can be described mathematically. Mechanics and CO₂ elimination can straightforwardly be described by simple mathematics. Furthermore, the parameters can be determined using a non-invasive fully automated technique as shown. In contrast, the effect of ventilator resetting on oxygenation is too complex to be modeled. Physiological parameters influencing oxygenation like cardiac output, right to left shunt and V/Q non-homogeneity can only be determined by invasive techniques. Accordingly, this study focussed on CO₂ elimination and ventilator pressure after resetting. Tidal volume and respiratory rate are important factors determining mechanical behavior and CO₂ elimination. These factors, which presently are in focus with respect to lung protective ventilation (16), were investigated in this first study of how simulations may be used to predict the results of alternative ventilator settings.

The simple model of lung physiology employed, allowed parameter estimation from normal breaths, only supplemented with a post-expiratory pause. The simple model also eased simulations. A model based upon a linear pressure volume curve without hysteresis and constant inspiratory resistance was applied. Studies in various mammals, healthy and diseased humans validate such a model as long as tidal volumes are not large (6, 7, 17–19). The model did not incorporate viscoelastic properties, as such properties are particularly difficult to measure (7, 20). Experimental validation is necessary to evaluate the adequacy of the simple model, the analysis leading to the physiological profile and the simulation program. The present study describes a method, illustrates its feasibility and serves as a first step in the validation that must be enlarged to lung disease and comprehensive variation in ventilator settings.

The method for simulation of mechanics was based upon calculation of events during small time intervals. This method allows simulation of any ventilator setting that can be described mathematically. The digital nature of the procedure made filters necessary in order to avoid oscillations originating from phase transitions. The method for simulation of CO₂ elimination was based upon a complete breath, with the V_T and RR as only input parameters.

Among the comprehensive results of each simulation P_{peak}, P_{plateau} and VCO₂ were selected for presentation, as these are particularly relevant with respect to lung protective ventilation. Data on mean airway

pressure and so-called auto-PEEP were not presented, as the settings studied in healthy pigs did not induce significant changes.

The differences between simulated and measured values at RR 20 reflect errors accumulated at measurements, modeling, parameterization and simulation. Measurement of VCO₂, which is based upon complete breaths is accurate. Modeling and parameterization are robust. As expected from these facts the simulation of VCO₂ was precise at RR 20. The errors in P_{plateau} and P_{peak} simulated at RR 20, were below 4% of measured values. This magnitude of errors is inherent to the methodological chain, from measurement to simulation. Simulation errors can not be expected to be less after resetting. After resetting to alternative values of RR and V_T the errors of simulation were not significantly larger. The small random deviations between simulated and measured pressures after resetting of the ventilator imply that the model, the parameterization and simulation from a mechanical point of view was adequate in the present context.

The systematic overestimation of CO₂ elimination at RR 25 and 30 probably reflects that time for gas mixing in the respiratory zone becomes too short for establishment of diffusion equilibrium. A longer time for gas mixing leads to lower airway dead space because of movement towards the airway opening by diffusion of the interface between alveolar and airway gas (21, 22). This feature is not taken into account in the present simulation program. Errors of 3 and 5% of simulated CO₂ elimination will lead to reciprocal changes in PaCO₂ after an equilibration time of roughly 20 min (3). If such deviations are considered important, amendment of the model may be needed. Whether this can be accomplished according to some general rules or if the dependence of CO₂ elimination on gas mixing time must be studied in each subject remains to be investigated. If needed, the influence of gas mixing time on CO₂ elimination may be studied by changing RR, T₁ or post-inspiratory pause time at the time when other parameters are measured before simulation.

A novel technique based upon observations of physiology under essentially unperturbed ventilation allowed prediction of CO₂ elimination and airway pressure after resetting respiratory rate and minute ventilation in healthy pigs. In principle, it is feasible to predict effects of ventilator resetting on the basis of a physiological profile. Before systems can be applied clinically tests must be performed for a wide range of pathology and extended types of resetting. It is expected that a physiological model needs to be complemented.

Acknowledgment

We thank Valéria Perez de Sa for valuable assistance.

References

1. Reynolds EO. Effect of alterations in mechanical ventilator settings on pulmonary gas exchange in hyaline membrane disease. *Arch Dis Child* 1971; **46**: 152–159.
2. Jansson L and Jonson B. A theoretical study on flow patterns of ventilators. *Scand J Respir Dis* 1972; **53**: 237–246.
3. Taskar V, John J, Larsson A, Wetterberg T and Jonson B. Dynamics of carbon dioxide elimination following ventilator resetting. *Chest* 1995; **108**: 196–202.
4. Svantesson C, Drefeldt B, Sigurdsson S, Larsson A, Brochard L and Jonson B. A Single Computer-Controlled Mechanical Insufflation Allows Determination of the Pressure-Volume Relationship of the Respiratory System. *J Clin Monitoring Computing* 1999; **15**: 9–16.
5. Fletcher R, Werner O, Nordstrom L and Jonson B. Sources of error and their correction in the measurement of carbon dioxide elimination using the Siemens-Elema CO₂ Analyzer. *Br J Anaesth* 1983; **55**: 177–185.
6. Liu JM, De Robertis E, Blomquist S, Dahm PL, Svantesson C and Jonson B. Elastic pressure-Volume curves of the respiratory system reveal a high tendency to lung collapse in young pigs. *Intensive Care Med* 1999; **25**: 1140–1146.
7. Jonson B, Beydon L, Brauer K, Månsson C, Valind S and Grytzell H. Mechanics of respiratory system in healthy anesthetized humans with emphasis on viscoelastic properties. *J Appl Physiol* 1993; **75**: 132–140.
8. Svantesson C, John J, Taskar V, Evander E and Jonson B. Respiratory mechanics in rabbits ventilated with different tidal Volumes. *Respir Physiol* 1996; **106**: 307–316.
9. Briscoe WA and Dubois AB. The relationship between airway resistance, airway conductance and lung Volume in subjects of different age and body size. *J Clin Invest* 1958; **37**: 1279–1285.
10. Rohrer F. Der Strömungswiderstand in den menschlichen Atemwegen und der Einfluss der unregelmässigen Verzweigung des Bronchialsystems auf den Atmungsverlauf. *Archiv für die Gesamte Physiologie* 1915; **162**: 225–299.
11. Eriksson L, Wollmer P, Olsson CG et al. Diagnosis of pulmonary embolism based upon alveolar dead space analysis. *Chest* 1989; **96**: 357–362.
12. Åström E, Niklason L, Drefeldt B, Bajc M and Jonson B. Partitioning of dead space – a method and reference values in the awake human. *Eur Respir J* 2000; **16**: 659–664.
13. Fletcher R and Jonson B. Dead-space and the single breath test for carbon dioxide during anaesthesia and artificial ventilation. Effects of tidal Volume and frequency of respiration. *Br J Anaesth* 1984; **56**: 109–119.
14. Morgenstern U and Kaiser S. Mathematical modelling of ventilation mechanics. *Int J Clin Monit Comput* 1995; **12**: 105–112.
15. Winkler T, Krause A and Kaiser S. Simulation of mechanical respiration using a multicompartiment model for ventilation mechanics and gas exchange. *Int J Clin Monit Comput* 1995; **12**: 231–239.
16. The Acute Respiratory Distress Syndrome Network. Ventilation with lower tidal Volumes as compared with traditional tidal Volumes for acute lung injury and the acute respiratory distress syndrome. *N Engl J Med* 2000; **342**: 1301–1308.
17. Gottfried SB, Rossi A, Calverley PM, Zocchi L and Milic-Emili J. Interrupter technique for measurement of respiratory mechanics in anesthetized cats. *J Appl Physiol* 1984; **56**: 681–690.
18. Similowski T, Levy P, Corbeil C et al. Viscoelastic behavior of lung and chest wall in dogs determined by flow interruption. *J Appl Physiol* 1989; **67**: 2219–2229.
19. Beydon L, Svantesson C, Brauer K, Lemaire F and Jonson B. Respiratory mechanics in patients ventilated for critical lung disease. *Eur Respir J* 1996; **9**: 262–273.
20. Bates JH, Brown KA and Kochi T. Respiratory mechanics in the normal dog determined by expiratory flow interruption. *J Appl Physiol* 1989; **67**: 2276–2285.
21. Fowler WS. Lung function studies. II. The respiratory dead-space. *Am J Physiol* 1948; **154**: 405–416.
22. Bowes CL, Richardson JD, Cumming G and Horsfield K. Effect of breathing pattern on gas mixing in a model with asymmetrical alveolar ducts. *J Appl Physiol* 1985; **58**: 18–26.

Address:
Leif Uttman
Department of Clinical Physiology
University Hospital
SE-221 85 Lund
Sweden
Fax: +46 46 151769
e-mail: leif.uttman@klinikfys.lu.se

L. Beydon
L. Uttman
R. Rawal
B. Jonson

Effects of positive end-expiratory pressure on dead space and its partitions in acute lung injury

Received: 27 November 2001
Accepted: 17 June 2002
Published online: 27 July 2002
© Springer-Verlag 2002

Supported by the Swedish Medical Research Council (02872) and the Swedish Heart Lung Foundation

L. Beydon (✉) · R. Rawal
Department of Anaesthesia,
University Hospital,
49033 Angers Cedex 01, France
e-mail: lbeydon.angers@invivo.edu
Tel.: +33-2-41353951
Fax: +33-2-41355224

L. Uttman · B. Jonson
Department of Clinical Physiology,
University Hospital, 22185 Lund, Sweden

Abstract Objective: A large tidal volume (VT) and lung collapse and re-expansion may cause ventilator-induced lung injury (VILI) in acute lung injury (ALI). A low VT and a positive end-expiratory pressure (PEEP) can prevent VILI, but the more VT is reduced, the more dead space (VD) compromises gas exchange. We investigated how physiological, airway and alveolar VD varied with PEEP and analysed possible links to respiratory mechanics.

Setting: Medical and surgical intensive care unit (ICU) in a university hospital. **Design:** Prospective, non-randomised comparative trial.

Patients: Ten consecutive ALI patients. **Intervention:** Stepwise increases in PEEP from zero to 15 cmH₂O. **Measurements and results:** Lung mechanics and VD were measured at each PEEP level. Physiological VD was 41–64% of VT at zero PEEP and increased

slightly with PEEP due to a rise in airway VD. Alveolar VD was 11–38% of VT and did not vary systematically with PEEP. However, in individual patients a decrease and increase of alveolar VD paralleled a positive or negative response to PEEP with respect to oxygenation (shunt), respectively. VD fractions were independent of respiratory resistance and compliance.

Conclusions: Alveolar VD is large and does not vary systematically with PEEP in patients with various degrees of ALI. Individual measurements show a diverse response to PEEP. Respiratory mechanics were of no help in optimising PEEP with regard to gas exchange.

Keywords Artificial respiration · Pulmonary gas exchange · Respiratory dead space · Respiratory mechanics · Acute lung injury

Introduction

For a long time measurement of physiological dead space (VD_{phys}) and its partitioning into airway (VD_{aw}) and alveolar (VD_{alv}) dead space has been feasible at the bedside with fast responding systems measuring airway flow rate and expired CO₂ at airway opening, in combination with arterial blood gas analysis [1]. The technique applied, in the form of the single breath test for CO₂ (SBT-CO₂), has provided new insight into the ventilation of patients under anaesthesia [1, 2] and the pathophysiology and diagnostics of lung disease [3, 4].

In previous studies it has been shown that SBT-CO₂ may indicate the nature of the pathology, such as airway obstruction, vascular disease and embolism. In this field there is 25 years of experience in anaesthesia, but little information is available in intensive care. However, little is known about the magnitude of dead space (VD) and its fractions airway dead space (VD_{aw}) and alveolar dead space (VD_{alv}) in acute lung injury (ALI) and acute respiratory distress syndrome (ARDS). Quantitative studies of how positive end-expiratory pressure (PEEP) affects these parameters are lacking, although Suter et al., in a pioneering study, reported that the best PEEP corre-

Table 1 Patient characteristics and status at zero end-expiratory pressure

Subject no.	Age (years)	Height (cm)	Weight (kg)	Cause of acute respiratory failure	Lung Injury Score*	Compliance (ml/cmH ₂ O)	PaO ₂ /FIO ₂ (mmHg)	Days of ventilation
1	55	170	80	Multiple trauma including chest	2.75	39	67	1
2	31	173	67	Near drowning	2.75	36	72	1
3	19	183	78	Haemoptysis	2.50	32	81	2
4	72	183	76	Cardiogenic oedema	1.75	42	267	16
5	67	172	70	Cardiogenic oedema	2.25	44	118	5
6	74	180	70	Pneumonia	2.50	40	53	1
7	66	178	72	Aortic dissection, postoperative	1.50	36	265	4
8	43	172	69	Cirrhosis, oesophageal bleeding	2.50	38	166	4
9	53	162	60	Cardiogenic oedema + coronary disease	2.50	29	127	10
10	34	177	74	Multiple trauma including chest	2.25	36	192	19

*Reference 12

sponded to the lowest VD and highest compliance [5]. Blanch et al. found no effect of PEEP on the Bohr dead space [6]. Later, Shimada et al. showed how VD varies with time in ARDS [7]. Measurements of the arterial to end-tidal PCO₂ gradient in ALI and ARDS to optimise ventilation have been confined to animal studies [8].

Ventilation at low tidal volume (VT) has been emphasised as an important component in lung protective ventilation [9]. In some patients CO₂ retention leading to respiratory acidosis was partly counteracted by increasing the respiratory rate (RR). However, VD ventilation limits the degree to which this can be achieved. Basal knowledge about VD and its fractions and how it varies with PEEP is needed for further understanding of how ventilation may be optimised in severe lung disease.

The goal of the present study was to quantify VD_{phys} and its partitions VD_{aw} and VD_{alv} in patients with varying lung pathology mechanically ventilated for ALI and assess the response to PEEP. Similarly, respiratory mechanics were studied [10] to identify possible links between VD and lung mechanics [5].

Methods

Material

Approval of the ethics committee and informed consent were obtained from the subjects' next of kin. Ten consecutive patients in stable haemodynamic and respiratory condition ventilated for ALI (PaO₂/FIO₂ ≤ 300 mmHg at inclusion) were studied supine. Patient characteristics and status at the start of measurement, i.e. at zero end-expiratory pressure (ZEEP), are given in Table 1. The subjects were sedated with fentanyl (5 µg/kg in bolus and then 5 µg/kg per h) and midazolam (0.05 mg/kg in bolus and then 0.05 mg/kg per h). Paralysis was maintained during the study with pancuronium bromide (0.10 mg/kg in bolus and then 0.10 mg/kg per h). The baseline ventilator setting was constant inspiratory flow, RR 17 ± 1.7 min, inspiratory time 33%, post-inspiratory pause 20% and ZEEP. FIO₂ was 1.0. The CO₂ Analyzer 930 (Siemens-Elema, Solna, Sweden) and the humidifying filter with connector contributed to VD_{aw} by 100 ml.

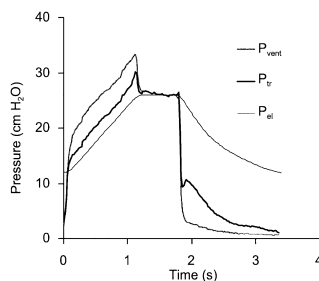


Fig. 1 Recorded pressure measured in the expiratory line of the ventilator (P_{vent}), calculated tracheal pressure (P_{tr}) and elastic recoil pressure (P_{el}) during a breath in patient 1 at positive end-expiratory pressure (PEEP) 0 cmH₂O. This patient had a very high auto-PEEP

Protocol

Ten breaths were recorded [11] and blood gases measured at ZEEP and at PEEP 2.5, 5, 7.5, 10 and 15 cmH₂O. Each PEEP level was maintained for 10 min before recordings.

Data analysis

Signal analysis [12] assumed constant inspiratory resistance (R_i) and compliance (C), zero elastic hysteresis [12, 13], expiratory conductance (G_E) linearly variable with volume [14] and flow-dependent tube resistance [15]. Tracheal pressure (P_{tr}) was calculated by subtracting the tube resistive pressure. Post-inspiratory elastic recoil pressure (P_{plat}) was read after the 0.7 s long post-inspiratory pause (Fig. 1). C was calculated from the slope of P_{tr} versus volume (compare with [16]). The course of the elastic recoil pressure (P_{el}) during the breath was determined from P_{plat} , C and volume. R_i was calculated as the quotient between average ($P_{tr} - P_{el}$) and airway flow rate (V'_{aw}) during the period of constant inspiratory flow. G_E was calculated as the quotient between V'_{aw} and ($P_{tr} - P_{el}$) for each sampling period over the segment covering 15–85% of VT. The relationship between G_E and volume was determined by regression. Expiratory resistance (R_E) was then calcu-

Table 2 Gas exchange and mechanics (R_i inspiratory resistance, $R_{E15\%VT}$, $R_{E50\%VT}$, $R_{E85\%VT}$ expiratory resistance at 15, 50 and 85% of VT, respectively)

PEEP (cmH ₂ O)	PaCO ₂ (mmHg) Average (SD)	PaO ₂ (mmHg) Average (SD)	R _i (cmH ₂ O/l per s) Average (SD)	R _{E15%VT} (cmH ₂ O/l per s) Average (SD)	R _{E50%VT} (cmH ₂ O/l per s) Average (SD)	R _{E85%VT} (cmH ₂ O/l per s) Average (SD)	Compliance (ml/cmH ₂ O) Average (SD)
0	44.7 (10.8)	148 (105)	9.5 (4.6)	26.0 (20.9)	18.5 (9.1)	16.7 (5.1)	37 (5)
2.5	44.9 (10.1)	134 (94)	8.2 (4.7)	21.2* (16.7)	15.7* (8.3)	15.1 (4.0)	38 (4)
5	44.3 (9.6)	141 (98)	7.7* (5.1)	17.7* (12.5)	14.6* (6.9)	15.0 (3.3)	37 (5)
7.5	45.0 (10.7)	142 (93)	6.6* (4.8)	14.5* (7.6)	13.2* (5.5)	14.8 (4.2)	36 (4)
10	44.7 (10.4)	150 (93)	6.1* (4.9)	12.7* (5.7)	12.8* (4.7)	15.3 (4.1)	34* (4)
15	44.3 (9.7)	173 (93)	5.6* (4.0)	9.8* (2.9)	11.4* (2.9)	15.6 (4.5)	30* (4)

* $p < 0.05$, t -test relative to ZEEP

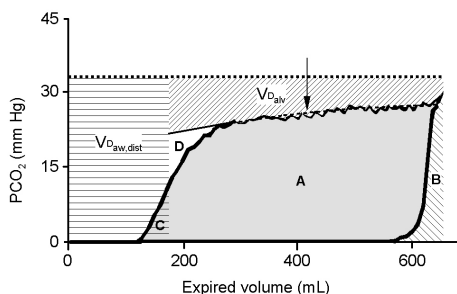


Fig. 2 In the single breath test for carbon dioxide (CO_2) the amount of CO_2 eliminated corresponds to area A within the loop depicting partial pressure of airway CO_2 ($P_{aw}CO_2$) versus volume. Airway dead space distal to the CO_2 sensor is indicated by the horizontally hatched area ($VD_{aw, dist}$). Airway dead space proximal to the sensor is indicated by hatched area B representing re-inspired CO_2 . Alveolar dead space is illustrated by the hatched area marked VD_{alv} between the extrapolated alveolar plateau and $PaCO_2$ (heavy interrupted line). The mode of calculation of VD_{alv} implies that the triangles C and D are of equal size. Arrow indicates the volume at which the slope of the alveolar plateau was calculated

lated as G_E^{-1} at volumes corresponding to 15, 50 and 85% of VT ($R_{E15\%VT}$, $R_{E50\%VT}$, $R_{E85\%VT}$).

Dead space partitions were calculated as percents of VT. Signals for V_{aw} (BTPS) and partial pressure of CO_2 in the airway ($P_{aw}CO_2$) were analysed to yield the single breath test for CO_2 (SBT- CO_2) (Fig. 2) [17]. The loop depicting PCO_2 versus volume (area A) reflects tidal CO_2 elimination. Hence:

$$VD_{phys} = (PaCO_2 \cdot VT - \text{area A}) / (PaCO_2 \cdot VT) \cdot 100 \quad (1)$$

Airway VD distal to the CO_2 sensor ($VD_{aw, dist}$) was determined according to an algorithm of Wolff and Brunner [18] that was modified to correct for a sloping alveolar plateau [19] in accordance with principles previously described [20].

Carbon dioxide re-inspired from the proximal airway dead space ($VD_{aw, prox}$) corresponds to area B (Fig. 2):

$$VD_{aw, prox} = \text{area B} / (PaCO_2 \cdot VT) \cdot 100 \quad (2)$$

$$VD_{alv} = VD_{phys} - (VD_{aw, prox} + VD_{aw, dist}) \quad (3)$$

The alveolar plateau was described in an equation [19] from which the slope of the alveolar plateau (SLOPE) at the volume halfway

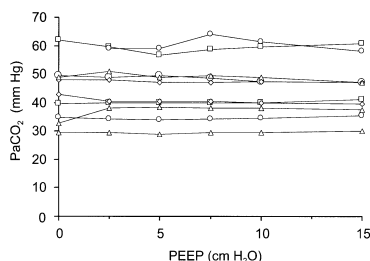


Fig. 3 Arterial partial pressure of carbon dioxide ($PaCO_2$) at different positive end-expiratory pressure (PEEP) levels in each subject

between $VD_{aw, dist}$ and VT was calculated (Fig. 2). Average values were calculated from the regular breaths recorded.

Statistical methods

The data are presented as averages \pm SD. Two-way ANOVA was used to analyse variations with PEEP, complemented with Student's paired two-tailed t -test. Orthogonal linear regressions were applied to identify relationships between the partitions of VD , alveolar slope or PaO_2 changes with PEEP and combinations of two variables among, e.g. R_i , R_E , C and lung injury score (LIS) [21]. A p value less than 0.05 was considered significant.

Results

Ventilation

At ZEEP and at all PEEP levels, the average VT was 623–629 ml and showed no tendency to vary with PEEP. At a PEEP of 15 cmH₂O, the average plateau pressure was 36 cmH₂O (range 28–44). Average $PaCO_2$ varied between 44.3 and 45.0 mmHg at different PEEP levels (Table 2). $PaCO_2$ for individual subjects showed only minor non-systematic variations with PEEP (Fig. 3). In the whole group of patients, PaO_2 did not vary significantly with PEEP (Table 2). Linear regression between

Table 3 Dead space values and mid-alveolar plateau slope (VD_{phys} physiological dead space, $VD_{aw,tot}$ total airway dead space, VD_{alv} alveolar dead space)

PEEP (cmH ₂ O)	$V_{d,phys}$ (% V_T) Average (SD)	$VD_{aw,tot}$ (% V_T) Average (SD)	VD_{alv} (% V_T) Average (SD)	Mid-alveolar plateau slope (mmHg/100 ml) Average (SD)
0	52.7 (8.7)	29.9 (4.6)	23.1 (8.6)	2.6 (1.0)
2.5	53.3 (8.2)	29.8 (4.9)	23.4 (8.2)	2.5 (1.0)
5	53.2 (7.9)	30.2 (4.9)	22.9 (7.7)	2.5 (1.0)
7.5	54.1* (7.5)	31.0* (4.8)	23.2 (8.1)	2.5 (1.0)
10	54.5 (6.8)	31.8* (4.8)	22.7 (7.7)	2.4 (1.1)
15	55.7 (6.6)	32.8* (5.2)	23.0 (8.1)	2.4 (1.1)

* $p < 0.05$

t -test relative to ZEEP

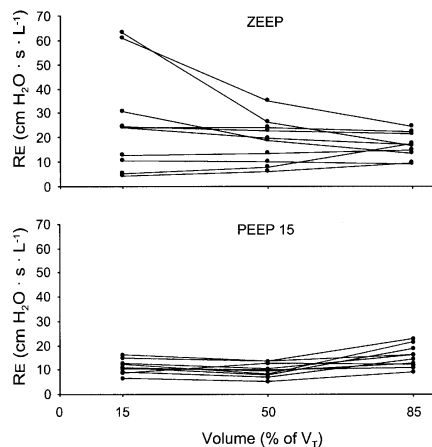


Fig. 4 Expiratory resistance (R_E) at the beginning, middle and end of expiration in each subject at zero end-expiratory pressure (ZEEP; upper panel) and at positive end-expiratory pressure (PEEP 15; lower panel)

PaO_2 and PEEP within subjects showed a significant increase in PaO_2 with increasing PEEP in four subjects ($r \geq 0.79$), which indicates a reduced shunt caused by recruitment. The opposite trend was significant in two subjects ($r \leq -0.75$).

Respiratory mechanics

Inspiratory resistance decreased significantly with PEEP ($R_I = -0.27$ PEEP + 9.0, $p = 0.002$) (Table 2). At ZEEP, the R_E measured at mid-expiration ($R_{E50\%VT}$) was higher than R_I ($p = 0.002$). $R_{E50\%VT}$ decreased significantly with PEEP ($p < 0.001$). At ZEEP, R_E towards the end of expiration ($R_{E15\%VT}$) was high in six subjects in whom it was much reduced at PEEP 15 (Fig. 4, compare upper and lower panels). The resistance at the beginning of expiration ($R_{E85\%VT}$) did not vary with PEEP (Table 2, Fig. 4). At PEEP 15 resistance decreased during expiration ($p < 0.001$), in contrast to the increase observed at ZEEP ($p < 0.001$).

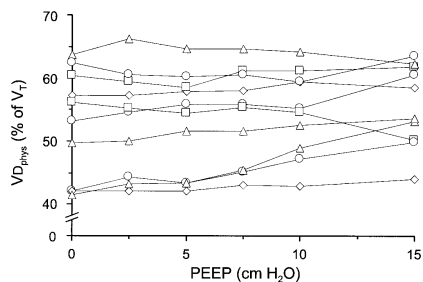


Fig. 5 Physiological dead space (VD_{phys}) at different positive end-expiratory pressure (PEEP) levels in each subject

Compliance at ZEEP varied between 29 and 44 ml/cmH₂O. C decreased with PEEP ($p < 0.001$). The decrease was confined to PEEP 10 and 15 (Table 2).

Carbon dioxide and dead space measurement

Typical features of the SBT-CO₂ are shown in Fig. 2. $VD_{aw,dist}$, which incorporates the humidifying filter, was 163 ± 23 ml at ZEEP, while the average $VD_{aw,prox}$ was 20 ± 5.5 ml. Accordingly, total airway VD ($VD_{aw,tot}$) was 183 ± 26 ml. At ZEEP average $VD_{aw,tot}$ was $30 \pm 5\%$ of VT and increased significantly to $33 \pm 5\%$ at PEEP 15 (Table 3). This increase in $VD_{aw,tot}$ was closely correlated with the concurrent increase in mean P_{tr} from 8.3 to 15.3 cmH₂O ($r = 0.98$, $p < 0.001$). The average VD_{alv} was $23 \pm 9\%$ of VT at ZEEP. VD_{alv} did not change significantly with PEEP (Table 3).

The change in PaO_2 with PEEP and the change in VD_{alv} with PEEP in individual patients were quantified from the slopes of the corresponding linear regressions. These slopes were correlated significantly with one another ($r = -0.78$, $p = 0.01$). This indicates that a positive or negative change in PaO_2 with PEEP in individual patients was coupled to an opposite change in VD_{alv} . A similar tendency was found if VD_{alv} was replaced by VD_{phys} ($r = -0.57$, $p = 0.05$).

The slope of the alveolar plateau at ZEEP (SLOPE_{ZEEP}) was, on average, 2.6 ± 1.0 mmHg/100 ml (range 1.6–4.5)

(Table 3). SLOPE did not vary significantly with PEEP in the whole group of patients. SLOPE_{ZEEP} correlated with R_1 (SLOPE_{ZEEP} = $0.15 \times R_1 + 1.19$, $p=0.03$), but not significantly with $R_{E50\%VT}$ ($p=0.1$).

The average VD_{phys} was $53 \pm 9\%$ of VT at ZEEP or, corrected for the dead space of the CO_2 analyser, filter and connector, $36 \pm 7\%$. The range was similarly wide at all PEEP levels (Fig. 5). Although the change in VD_{phys} with PEEP was slight in each subject (Fig. 5), ANOVA showed a slight increase with PEEP ($p=0.02$). The increase was of the same magnitude as that of VD_{aw} (Table 3). Neither partitions of VD nor PaO_2 changes with PEEP showed significant correlation to mechanical parameters such as R_1 , R_E or C, or with combinations of these parameters. VD_{alv} at ZEEP tended to correlate with LIS ($VD_{alv} = 11.2 \times LIS - 2.7$, $p=0.07$).

Discussion

Our main findings are that VD_{alv} is large and does not vary systematically with PEEP in patients with various degrees of ALI. However, subjects in whom oxygenation improved with PEEP showed a concurrent decrease in VD_{alv} and vice versa. There was a positive trend between VD_{alv} and LIS.

The intention to study patients with various degrees of lung injury was met, as shown by the variation of C, R and VD from nearly normal to highly pathological values. A large increase in R_E during expiration at ZEEP has previously been reported for patients with severe airflow obstruction [22]. In some of our patients similar findings may reflect further narrowing of obstructed airways, airway closure at low lung volume or both [13, 23]. That R_E at high PEEP was higher during early expiration than later has previously been observed with the flow interruption technique [13]. This may indicate overstretching of lung and airways. R_1 was lower at higher PEEP, perhaps due to both airway distension and the recruitment of airways closed at low PEEP.

When alveolar ventilation is changed, it takes 15–30 min to establish a new steady state with respect to CO_2 turnover [24]. A stable $PaCO_2$ in each patient indicated steady state, a prerequisite for dead space analysis. Hence, 10 min of ventilation at each PEEP level was adequate. To avoid a possible perturbation of physiological status induced by high levels of PEEP, the sequence of PEEP levels was not varied randomly.

According to principles of Fowler [25], Fletcher et al. developed the SBT- CO_2 for simple VD analysis [17]. We complemented the classical SBT- CO_2 by its inspiratory limb, so as to measure the re-inspired volume of CO_2 resident in the Y-piece and ventilator lines and to calculate $VD_{aw,prox}$. The magnitude of $VD_{aw,prox}$ that, in part, reflects gas mixing in the ventilator lines was similar to previous data [26]. $VD_{aw,disst}$, corrected for the dead space of the filter and CO_2 analyser, was 63 ± 23 ml. Our values

are 71% of those Fletcher et al. found in patients anaesthetised for general surgery [1]. The difference may be of a methodological nature. We applied the principle of Wolff and Brunner [18] that is considered to give "the smallest possible of determinable values of airway dead space" [19]. Fletcher used the original principle of Fowler [25] that probably gives higher values because correction for the alveolar slope, that decreases the airway dead space calculated [20], was not performed. High airway pressure induced by PEEP increased VD_{aw} as previously observed [27].

Alveolar VD depends on several factors, including age, VT, ventilation/perfusion ratio (V/Q), flow wave pattern and airway pressure [5, 17, 19]. In the SBT- CO_2 , VD_{alv} is recognised from a large difference between $PaCO_2$ and the alveolar plateau. This difference can be discussed either in terms of an elevation of $PaCO_2$ or a depression of the alveolar plateau.

In ARDS the elevation of $PaCO_2$ in relation to alveolar gas is mainly caused by an intrapulmonary shunt leading to venous admixture to arterialised blood. The importance of shunt was corroborated by inverse changes in PaO_2 and VD_{alv} when PEEP was changed. As early as 1973 McMahon et al. observed that patients who respond to PEEP with an increase in PaO_2 also respond with a fall in VD [28]. The opposite effect of PEEP may reflect a diversion of blood flow towards collapsed areas [29]. Another factor may be haemodynamic changes attributable to the combined effects of reduced preload and raised juxta-cardiac pressure resulting in a reduced ventricular filling pressure [30, 31]. Blanch et al. showed that the arterial to end-tidal CO_2 gradient had a minimum at a PEEP corresponding to the lower inflexion point of the elastic pressure volume curve [32]. In infants with hyaline membrane disease the arterial-mixed alveolar CO_2 gradient was minimal at the optimal level of continuous positive airway pressure [33]. These findings imply that VD_{alv} decreased when lung recruitment occurred. Our material, comprising a few patients with ARDS, revealed a clearly defined minimum of the arterial to end-tidal CO_2 gradient only for patient 2 (PEEP 5 cmH_2O). This is in conformity with Jardin et al., who found that the arterial to end-tidal CO_2 gradient did not permit exact titration of PEEP in acute respiratory insufficiency [34].

In positive PEEP responders the reduction of VD_{alv} compensated for the concurrent increase of VD_{aw} . In others the negative effects of PEEP on VD_{aw} and VD_{alv} were additive. For example, increasing PEEP by 10 cmH_2O led to an increase in VD_{aw} of 4.2% of VT and in VD_{alv} of 3.2% of VT in patient 4. To compensate for this, VT would need to be increased by 9%. This would not be trivial in a situation where VT should be restricted to about 6 ml/kg body weight [9]. In attempts to reduce VT and airway pressure, therefore, not only mechanical strain on the lung but also gas exchange and VD should be considered.

A depression of the alveolar plateau in relation to PaCO₂ reflects uneven V/Q. Then, CO₂-rich gas from well-perfused compartments is diluted by gas from poorly or non-perfused compartments. Vasoconstriction and microvascular thrombosis lead to such effects in ALI and ARDS [35]. When uneven V/Q is caused by vascular pathology, the depressed alveolar plateau will remain nearly flat because different lung compartments empty synchronously [36]. In contrast, airway obstruction leads to an increased slope of the alveolar plateau caused by sequential emptying of lung compartments with different V/Qs [17]. Blanch et al. [37] observed an association between auto-PEEP and the alveolar slopes in capnograms (mmHg/s). Auto-PEEP probably reflected airway obstruction in their patients. In a later study from the same group [6], an association between the alveolar slope and LIS was observed in patients with ALI and ARDS. In dogs with oleic acid-induced ARDS, the PEEP associated with the lowest arterial to end-tidal PCO₂ gradient was considered to reflect the optimal PEEP at which oxygen delivery was highest [8]. Compliance did not help to find the optimal PEEP. These results are consistent with ours.

Comparisons with previous data for VD_{phys} are compromised by differences in technique and unclear notation about apparatus VD in some publications. Our data appear somewhat lower than those reported by Feihl et al. and Hoffman et al. [38, 39]. Differences are partly explained by lower degrees of lung injury in our patients. Our data overlap with observations in anaesthetised, ventilated subjects without primary lung disease [40, 41]. The small effect of PEEP on VD_{phys} found in our study is fully explained by the effect on VD_{aw}. Accordingly,

PEEP had no systematic effect on alveolar V/Q non-homogeneity leading to effects on VD. This is in conformity with observations by Ralph et al. [42], who found no correlation between PEEP and inert gas VD. Coffey et al. [43] found, in oleic acid-induced ARDS, that low PEEP reduced VD_{phys} because of the reduced shunt. A high PEEP increased VD_{phys} by increasing the fraction of ventilation delivered to areas with a high V/Q. We did not observe such a bimodal effect of PEEP.

Lung protective ventilation relies much upon low tidal volumes [9]. A reduction of VD_{aw} and VD_{phys} is therefore of potential value. VD_{aw} can be reduced by replacing passive humidifiers of inspired gas with active ones [44, 45]. VD_{aw} can also be reduced by tracheal gas insufflation [46] and aspiration of VD [47]. These methods have limited availability. About 20 ml of VD reflects CO₂ present in the ventilator tubing close to the Y-piece at the start of inspiration [26]. In some ventilators a continuous bypass flow during expiration facilitates the triggering of inspiration [48]. Such a bypass flow must wash out at least some of this VD, but this has not been studied. The effect of ventilator resetting on VD_{phys} is not predictable. The SBT-CO₂, when recorded in a particular patient, illustrates the importance of VD and allows follow-up of a new setting.

We conclude that the awareness of large VD fractions illustrated in this study is important in protective ventilation strategies. The issue of how to reduce VD is complex, as reflected by the diverse response to PEEP, which we could recognise because of the various degrees of lung injury. Respiratory mechanics were of no help in optimising PEEP with regard to gas exchange. Studies in more specific groups of patients are now required.

References

- Fletcher R, Jonson B (1984) Dead space and the single breath test for carbon dioxide during anaesthesia and artificial ventilation. Effects of tidal volume and frequency of respiration. *Br J Anaesth* 56:109–119
- Malmkvist G, Fletcher R, Jonson B, Jansson L (1985) On-line dead space measurement during cardiac surgery. *Clin Physiol* 5 (Suppl 3):147–148
- Olsson K, Jonson B, Olsson CG, Wollmer P (1998) Diagnosis of pulmonary embolism by measurement of alveolar dead space. *J Intern Med* 244:199–207
- Jonsson H, Nived O, Sturfelt G, Valind S, Jonson B (1989) Lung function in patients with systemic lupus erythematosus and persistent chest symptoms. *Br J Rheumatol* 28:492–499
- Suter PM, Fairley B, Isenberg MD (1975) Optimum end-expiratory airway pressure in patients with acute pulmonary failure. *N Engl J Med* 292:284–289
- Blanch L, Lucangelo U, Lopez-Aguilar J, Fernandez R, Romero PV (1999) Volumetric capnography in patients with acute lung injury: effects of positive end-expiratory pressure. *Eur Respir J* 13:1048–1054
- Shimada Y, Yoshiya I, Tanaka K, Sone S, Sakurai M (1979) Evaluation of the progress and prognosis of adult respiratory distress syndrome. Simple respiratory physiologic measurement. *Chest* 76:180–186
- Murray IP, Modell JH, Gallagher TJ, Banner MJ (1984) Titration of PEEP by the arterial minus end-tidal carbon dioxide gradient. *Chest* 85:100–104
- The Acute Respiratory Distress Syndrome Network (2000) Ventilation with lower tidal volumes as compared with traditional tidal volumes for acute lung injury and the acute respiratory distress syndrome. *N Engl J Med* 342:1301–1308
- Uttman L, Jonson B (2002) Computer-aided ventilator resetting is feasible on the basis of a physiological profile. *Acta Anaesthesiol Scand* 46:289–296
- Svantesson C, Drefeldt B, Sigurdsson S, Larsson A, Brochard L, Jonson B (1999) A single computer-controlled mechanical insufflation allows determination of the pressure-volume relationship of the respiratory system. *J Clin Monit Comput* 15:9–16

12. Jonson B, Beydon L, Brauer K, Månsson C, Valind S, Grytzell H (1993) Mechanics of respiratory system in healthy anesthetized humans with emphasis on viscoelastic properties. *J Appl Physiol* 75:132–140
13. Beydon L, Svantesson C, Brauer K, Lemaire F, Jonson B (1996) Respiratory mechanics in patients ventilated for critical lung disease. *Eur Respir J* 9:262–273
14. Briscoe WA, Dubois AB (1958) The relationship between airway resistance, airway conductance and lung volume in subjects of different age and body size. *J Clin Invest* 37:1279–1285
15. Rohrer F (1915) Der Strömungswiderstand in den menschlichen Atemwegen und der Einfluss der unregelmässigen Verzweigung des Bronchialsystems auf den Atmungsverlauf. *Arch gesamte Physiol* 162:225–299
16. Ranieri VM, Zhang H, Mascia L, Aubin M, Lin CY, Mullen JB, Grasso S, Binnie M, Volgyesi GA, Eng P, Slutsky AS (2000) Pressure-time curve predicts minimally injurious ventilatory strategy in an isolated rat lung model. *Anesthesiology* 93:1320–1328
17. Fletcher R, Jonson B, Cumming G, Brew J (1981) The concept of dead space with special reference to the single breath test for carbon dioxide. *Br J Anaesth* 53:77–88
18. Wolff G, Brunner JX (1984) Series dead space volume assessed as the mean value of a distribution function. *Int J Clin Monit Comput* 1:177–181
19. Åström E, Niklason L, Drefeldt B, Bajc M, Jonson B (2000) Partitioning of dead space – a method and reference values in the awake human. *Eur Respir J* 16:659–664
20. Wolff G, Brunner JX, Weibel W, Bowes CL, R MWB (1989) Anatomical serial dead space volume; concept and measurement in clinical practice. *Appl Cardiopulm Pathol* 2:299–307
21. Murray JF, Matthay MA, Luce JM, Flick MR (1988) An expanded definition of the adult respiratory distress syndrome. *Am Rev Respir Dis* 138:720–723
22. Smith TC, Marini JJ (1988) Impact of PEEP on lung mechanics and work of breathing in severe airflow obstruction. *J Appl Physiol* 65:1488–1499
23. Eissa NT, Ranieri VM, Corbeil C, Chasse M, Braidy J, Milic-Emili J (1991) Effects of positive end-expiratory pressure, lung volume and inspiratory flow on interrupter resistance in patients with adult respiratory distress syndrome. *Am Rev Respir Dis* 144:538–543
24. Taskar V, John J, Larsson A, Wetterberg T, Jonson B (1995) Dynamics of carbon dioxide elimination following ventilator resetting. *Chest* 108:196–202
25. Fowler WS (1948) Lung function studies. II. The respiratory dead space. *Am J Physiol* 154:405–416
26. Fletcher R, Werner O, Nordström L, Jonson B (1983) Sources of error and their correction in the measurement of carbon dioxide elimination using the Siemens-Element CO₂ Analyzer. *Br J Anaesth* 55:177–185
27. Larsson A, Gilbert JT, Bunegin L, Gelineau J, Smith RB (1992) Pulmonary effects of body position, PEEP and surfactant depletion in dogs. *Acta Anaesthesiol Scand* 36:38–45
28. McMahon SM, Halprin GM, Sieker HO (1973) Positive end-expiratory airway pressure in severe arterial hypoxemia. *Am Rev Respir Dis* 108:526–535
29. Kanarek DJ, Shannon DC (1975) Adverse effect of positive end-expiratory pressure on pulmonary perfusion and arterial oxygenation. *Am Rev Respir Dis* 112:457–459
30. Marini JJ, Culver BH, Butler J (1981) Effect of positive end-expiratory pressure on canine ventricular function curves. *J Appl Physiol* 51:1367–1374
31. Potkin RT, Hudson LD, Weaver LJ, Trobaugh G (1987) Effect of positive end-expiratory pressure on right and left ventricular function in patients with the adult respiratory distress syndrome. *Am Rev Respir Dis* 135:307–311
32. Blanch L, Fernandez R, Benito S, Mancebo J, Net A (1987) Effect of PEEP on the arterial minus end-tidal carbon dioxide gradient. *Chest* 92:451–454
33. Landers S, Hansen TN, Corbet AJ, Stevens MJ, Rudolph AJ (1986) Optimal constant positive airway pressure assessed by arterial alveolar difference for CO₂ in hyaline membrane disease. *Pediatr Res* 20:884–889
34. Jardin F, Genevray B, Pazin M, Margairaz A (1985) Inability to titrate PEEP in patients with acute respiratory failure using end-tidal carbon dioxide measurements. *Anesthesiology* 62:530–533
35. Wort SJ, Evans TW (1999) The role of the endothelium in modulating vascular control in sepsis and related conditions. *Br Med Bull* 55:30–48
36. Eriksson L, Wollmer P, Olsson CG, Albrechtsson U, Larusdottir H, Nilsson R, Sjogren A, Jonson B (1989) Diagnosis of pulmonary embolism based upon alveolar dead space analysis. *Chest* 96:357–362
37. Blanch L, Fernandez R, Saura P, Baigorri F, Artigas A (1994) Relationship between expired capnogram and respiratory system resistance in critically ill patients during total ventilatory support. *Chest* 105:219–223
38. Feihl F, Eckert P, Brimiouille S, Jacobs O, Schaller MD, Melot C, Naeije R (2000) Permissive hypercapnia impairs pulmonary gas exchange in the acute respiratory distress syndrome. *Am J Respir Crit Care Med* 162:209–215
39. Hoffman LA, Miro AM, Tasota FJ, Delgado E, Zullo TG, Lutz J, Pinsky MR (2000) Tracheal gas insufflation. Limits of efficacy in adults with acute respiratory distress syndrome. *Am J Respir Crit Care Med* 162:387–392
40. Fletcher R, Jonson B (1981) Prediction of the physiological dead space/tidal volume ratio during anaesthesia/IPPV from simple pre-operative tests. *Acta Anaesthesiol Scand* 25:58–62
41. Puri GD, Singh H, Kaushik S, Jindal SK (1999) Physiological dead space during normocapnic ventilation under anaesthesia. *Anaesth Intensive Care* 27:159–163
42. Ralph DD, Robertson HT, Weaver LJ, Hlastala MP, Carrico CJ, Hudson LD (1985) Distribution of ventilation and perfusion during positive end-expiratory pressure in the adult respiratory distress syndrome. *Am Rev Respir Dis* 131:54–60
43. Coffey RL, Albert RK, Robertson HT (1983) Mechanisms of physiological dead space response to PEEP after acute oleic acid lung injury. *J Appl Physiol* 55:1550–1557
44. Campbell RS, Davis K Jr, Johannigman JA, Branson RD (2000) The effects of passive humidifier dead space on respiratory variables in paralyzed and spontaneously breathing patients. *Respir Care* 45:306–312
45. Richecoeur J, Lu Q, Vieira SR, Puybasset L, Kalfon P, Coriat P, Rouby JJ (1999) Expiratory washout versus optimization of mechanical ventilation during permissive hypercapnia in patients with severe acute respiratory distress syndrome. *Am J Respir Crit Care Med* 160:77–85
46. Jonson B, Similowski T, Levy P, Viies N, Pariente R (1990) Expiratory flushing of airways: a method to reduce dead space ventilation. *Eur Respir J* 3:1202–1205
47. De Robertis E, Servillo G, Tufano R, Jonson B (2001) Aspiration of dead space allows isocapnic low tidal volume ventilation in acute lung injury. *Intensive Care Med* 27:1496–1503
48. Aslanian P, El Atrous S, Isabey D, Valente E, Corsi D, Harf A, Lemaire F, Brochard L (1998) Effects of low triggering on breathing effort during partial ventilatory support. *Am J Respir Crit Care Med* 157:135–143

A prolonged post-inspiratory pause enhances CO₂ elimination by reducing airway dead space

LEIF UTTMAN AND BJÖRN JONSON

Department of Clinical Physiology, University Hospital, Lund, Sweden.

Abstract

CO₂ elimination per breath ($V_{CO_2,T}$) depends primarily on tidal volume (V_T). The time course of flow during inspiration influences distribution and diffusive mixing of V_T and is therefore a secondary factor determining gas exchange. To study the effect of a post-inspiratory pause we defined “mean distribution time” (MDT) as the mean time given to inspired gas for distribution and diffusive mixing within the lungs. The objective was to quantify changes in airway dead space (V_{Daw}), slope of the alveolar plateau (SLOPE) and $V_{CO_2,T}$ as a function of MDT in healthy pigs.

Methods: Ten healthy pigs were mechanically ventilated. Airway pressure, flow and partial pressure of CO₂ were recorded during resetting of the post-inspiratory pause *from* 10% (baseline) to, in random order, 0, 5, 20 and 30% of the respiratory cycle. The immediate changes in V_{Daw} , SLOPE, $V_{CO_2,T}$, and MDT after resetting were analysed.

Results: V_{Daw} in percent of V_T decreased from 29 to 22%, SLOPE from 0.35 to 0.16 kPa/100 mL as MDT increased from 0.51 to 1.39 s, respectively. Over the same MDT range, $V_{CO_2,T}$ increased by 10%. All these changes were statistically significant.

Conclusion: The time for gas distribution and diffusion affects gas exchange to such an extent that it may be of importance for optimisation of ventilator setting in severe lung disease.

Keywords: Pulmonary Gas Exchange, Respiratory Dead Space

INTRODUCTION

A low tidal volume (V_T) appears to be a crucial factor for lung protective ventilation in the acute respiratory distress syndrome. When low V_T is used to provide lung protective ventilation, respiratory acidosis may be partly balanced by an increased respiratory rate (RR) (1). In itself, a low V_T leads to increased dead space fraction. A short duration of inspiration that follows from an increased RR may then further compromise gas exchange by uneven distribution and inadequate mixing of V_T in the alveolar space. Different means to reduce dead space have been suggested. Examples are re-introduction of active humidifiers, tracheal gas insufflation and aspiration of dead space (2, 3). Another way to reduce dead space is to use a ventilator setting that enhances CO_2 elimination. Several studies in health or in disease show a decrease in dead space or PaCO_2 when using a post-inspiratory pause (4–8). However, positive effects of inspiratory patterns intended to improve gas exchange have not always been observed (6, 9–12). Partly diverging results may reflect methodological limitations. Recently, a known method allowing high accuracy of dead space determination in intensive care was further refined (13). A method to compensate for inevitable changes in V_T can be based on mathematical modelling of the alveolar plateau in the single breath test for CO_2 (SBT- CO_2) (14). In the present study we introduce the term “mean distribution time” (MDT), which is the mean time given to inspired gas for distribution and diffusive mixing within the lungs. MDT was varied by changing the duration of the post-inspiratory pause. The objective was to quantify changes in airway dead space (V_{Daw}), slope of the alveolar plateau (SLOPE) and CO_2 elimination per breath ($V_{\text{CO}_2,T}$) as a function of MDT in healthy pigs.

METHODS

Material

The local Ethics Board of Animal Research approved the experimental protocol. Ten pigs of the Swedish native breed, mean weight 29.5 kg (23.0–33.5), were fasted overnight with free access to water. Seven of these animals were the same as in (14). The animals were pre-medicated with azaperon ($7 \text{ mg}\cdot\text{kg}^{-1}$), anaesthetised with ketamin ($5 \text{ mg}\cdot\text{kg}^{-1}$), intubated with a 7.0 mm ID tracheal tube and connected to a ventilator (ServoVentilator 900C, Siemens-Elema, Solna, Sweden). The ventilator produced a square inspiratory flow pattern at a baseline setting of respiratory rate 20 min^{-1} , inspiratory time 33%, post-inspiratory pause time (T_P) 10% and positive end-expiratory pressure of 6 cm H_2O . The baseline minute ventilation was adjusted to achieve PaCO_2 4.5–5 kPa. A mainstream analyser (CO_2 Analyzer 930, Siemens-Elema, Solna, Sweden) measured partial pressure of CO_2 in expired and inspired gas (P_{CO_2}). Anaesthesia was maintained by continuous infusion of ketamin ($17 \text{ mg}\cdot\text{kg}^{-1}\cdot\text{h}^{-1}$), midazolam ($1.7 \text{ mg}\cdot\text{kg}^{-1}\cdot\text{h}^{-1}$) and pancuronium bromide ($0.5 \text{ mg}\cdot\text{kg}^{-1}\cdot\text{h}^{-1}$). The ventilator/computer system used for data recording has previously been described (15). Signals from the ventilator and CO_2 analyser representing flow rate, airway pressure and P_{CO_2} were sampled by a personal computer at the frequency of 50 Hz. Compliance of the tracheal tube and ventilator tubing was measured *in vitro*. There were no dropouts among the animals.

Protocol

After preparation of the pigs a stabilisation period of 30 min was allowed. A recruitment manoeuvre was performed by inflating the lungs with a pressure of 35 cm H₂O for 10 s to eliminate atelectasis and standardise lung volume history and conditions among the animals. The system was tested for leakage. A continuous record of a study sequence comprised the following elements: 10 normal breaths, 20 breaths of a different T_P, 10 normal breaths. T_P was changed by manual switch of the T_P control of the ventilator *from* 10 to 0, 5, 20 and 30% of the respiratory cycle, in randomised order.

Data analysis

Data sampled during a study sequence were transferred to a spreadsheet for analysis (Excel 97, Microsoft Corp., WA, USA). Measured flow rate was corrected for the compliance in the tubing in order to obtain airway flow rate (\dot{V}_{aw}). The expiratory flow signal was normalised by a correction factor so that expired volume equalled inspired volume. The correction factor obtained at T_P 10% was applied to all recordings. V_T was calculated by integration of expired \dot{V}_{aw} . Airway dead space distal to the CO₂ sensor was determined according to an algorithm of Wolff and Brunner (16) that was modified to correct for a sloping alveolar plateau (17) in accordance with principles previously described (18). Airway dead space distal to the tip of the tracheal tube (V_{Daw}) was calculated by subtracting the dead space volume of the tracheal tube and CO₂ analyser (16 mL). V_{CO₂T} was calculated as the difference between expired volume of CO₂ and that re-inspired from the Y-piece and adjacent tubing, which corresponds to the area within the

SBT-CO₂ loop (Figure 1) (14). From an equation describing the alveolar plateau its SLOPE was calculated at the volume halfway between V_{Daw} and V_T (13). Technical limitations and flux of gas from tubing to the subject in the first phase of a post-inspiratory pause caused small variations in V_T and thereby in V_{CO_{2,T}}. The effect on V_{CO_{2,T}} caused by V_T variation was not an issue of this study and was accordingly corrected for. How V_{CO_{2,T}} varies with V_T can be determined from the end-tidal alveolar slope and end-tidal P_{CO₂} in the SBT-CO₂ (14). V_{CO_{2,T}} was normalised to the lowest V_T observed as was end-tidal P_{CO₂}.

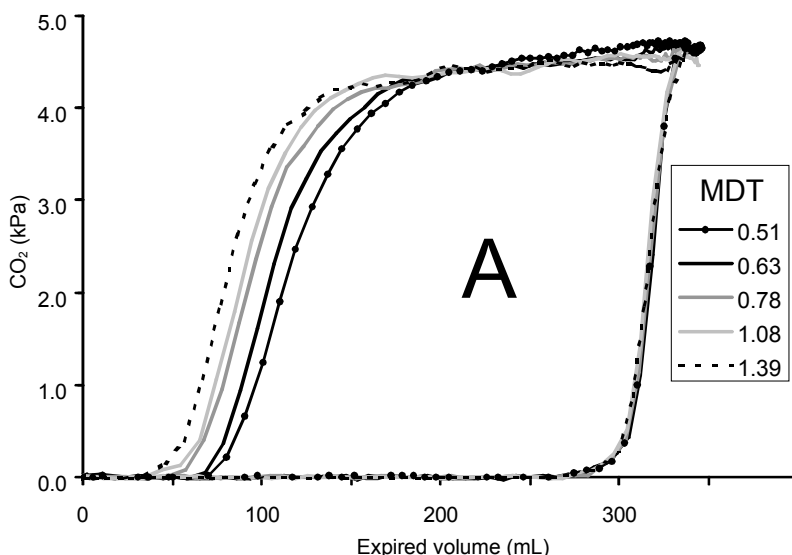


Figure 1. The single breath test for CO₂ in a representative animal at different mean distribution time (MDT). Longer MDT resulted in a left-hand shift of the sharp ascending expiratory limb of the loop. This corresponds to a decrease in airway dead space and an increase in tidal CO₂ elimination (area A). The slope of the alveolar plateau decreased with MDT.

For a certain pattern of inspiration including the post-inspiratory pause MDT was calculated from all samples during a recorded inspiration as:

$$\text{MDT} = \frac{\sum(\dot{V}_{\text{aw}} \cdot \Delta t \cdot t_{\text{dist}})}{\sum(\dot{V}_{\text{aw}} \cdot \Delta t)} = \frac{\sum(\dot{V}_{\text{aw}} \cdot t_{\text{dist}})}{\sum(\dot{V}_{\text{aw}})} \quad \text{Eq.1}$$

where Δt is the sampling interval (0.02 s) and t_{dist} is the time left for distribution of the particular gas sample until start of expiration.

Statistical methods

Data are presented as mean \pm SD. Two-way ANOVA was used to study variations of different parameters with MDT. Student's paired two-tailed t-test was used to analyse differences among parameters observed at MDT 0.51 s (T_P 0%) and other values of MDT.

RESULTS

V_T was 286 ± 42 mL, corresponding to 9.7 ± 1.0 mL \cdot kg $^{-1}$. V_T increased with on average 4 mL when T_P increased from 0 to 5% and remained at that level at longer T_P . The end-expiratory flow was 0 at T_P 0% to T_P 20% and increased to 0.05 ± 0.04 L \cdot s $^{-1}$ at T_P 30%. Plateau pressure measured at the end of the post-inspiratory pause showed only minor variations with T_P (Table 1).

Table 1. Consequences of post-inspiratory pause

T _P (%)	MDT (s)	V _{Daw} (% of V _T)	V _{CO₂T} (mL)	SLOPE		P _{CO₂ET} (kPa)	P _{plateau} (cm H ₂ O)
				Mean ± SEM	Mean ± SEM		
0	0.51 ± 0.01	29 ± 1.0	8.0 ± 0.57	0.35 ± 0.04	4.8 ± 0.12	--	--
5	0.63 ± 0.01	27 ± 0.9	8.1 ± 0.56	0.26 ± 0.02	4.7 ± 0.13	15.1 ± 0.5	15.1 ± 0.5
10	0.78 ± 0.01	25 ± 0.9	8.3 ± 0.59	0.24 ± 0.03	4.7 ± 0.12	14.8 ± 0.5	14.8 ± 0.5
20	1.08 ± 0.02	24 ± 0.9	8.6 ± 0.60	0.14 ± 0.01	4.7 ± 0.12	14.7 ± 0.5	14.7 ± 0.5
30	1.39 ± 0.02	22 ± 0.8	8.8 ± 0.60	0.16 ± 0.02	4.7 ± 0.14	15.0 ± 0.5	15.0 ± 0.5

MDT mean distribution time

V_{Daw} airway dead space

V_{CO₂T} tidal CO₂ elimination

P_{CO₂ET} end-tidal P_{CO₂}

P_{plateau} post-inspiratory plateau pressure

For the different T_P , MDT varied from 0.51–1.39 s with a coefficient of variation between pigs of less than 2% (Table 1). Figure 1 shows the SBT- CO_2 for the different MDT in a representative animal. As appears from Figure 2, V_{Daw} decreases non-linearly with MDT in each pig. The decrease in V_{Daw} resulted in an increase in $V_{CO_2,T}$ as illustrated in Figure 1.

Longer MDT led to lower SLOPE and lower end-tidal P_{CO_2} (ANOVA, $p < 0.001$ for both) (Table 1). Effects on $V_{CO_2,T}$, related to changes of the alveolar plateau, were calculated from changes in the area below the alveolar plateau. When T_P increased from 0 to 30% the observed changes of the alveolar plateau did not influence $V_{CO_2,T}$ ($p > 0.05$).

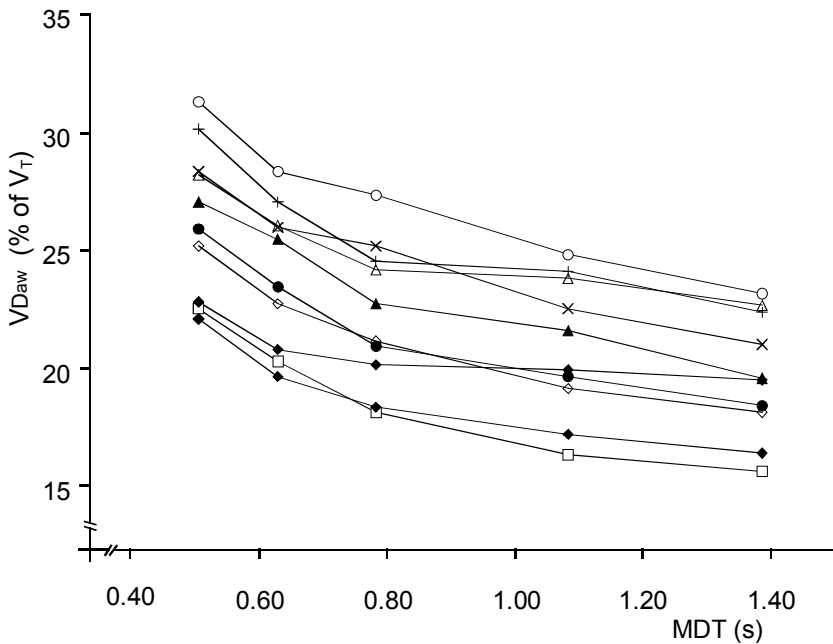


Figure 2. Airway dead space (V_{Daw}) as function of mean distribution time (MDT) in each subject.

When T_P increased from 0 to 30%, implying that MDT changed from 0.51 to 1.39 s, $V_{CO_2,T}$ in percent of the value at T_P 0% increased as shown in Figure 3. The change in $V_{CO_2,T}$ ($\Delta V_{CO_2,T}$) was expressed according to the equation:

$$\Delta V_{CO_2,T} = 7.24 + 10.6 \cdot \ln(MDT) \quad (r = 0.86, p < 0.001) \quad \text{Eq. 2}$$

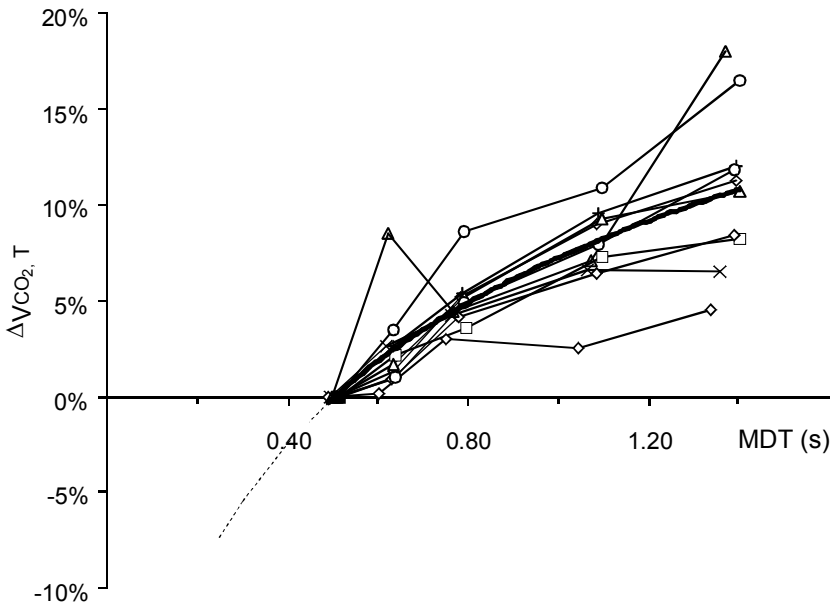


Figure 3. Tidal CO_2 elimination change ($\Delta V_{CO_2,T}$) as function of mean distribution time (MDT). Individual curves (thin drawn lines) and regression line (heavy line), with extrapolation (interrupted line).

DISCUSSION

This study shows that a post-inspiratory pause enhances CO₂ elimination by reducing V_{Daw} . The uniform results indicate that it is possible to detect even modest changes in V_{Daw} and CO₂ elimination. These changes follow immediately after resetting. In contrast, stabilisation of PaCO₂ following a change in CO₂ elimination takes several minutes (19, 20) and may be obscured by physiological instability. The determination of MDT according to Eq. 1 was robust as indicated by low scatter (Table 1).

Healthy pigs do not have collateral ventilation (21). Furthermore, different lung units probably fill and empty nearly synchronously. Obviously, the results cannot be applied on humans in whom collateral ventilation may equilibrate ventilation non-homogeneity, which may be of particular importance in obstructive lung disease.

The end-expiratory flow indicates the presence of auto-PEEP at T_p 30%. An estimate based on previous observations of expiratory resistance in healthy pigs (14) suggests that auto-PEEP was less than 0.5 cm H₂O. That auto-PEEP was unimportant was further supported by the nearly constant post-inspiratory plateau pressure (Table 1).

The algorithm of MDT (Eq. 1) dictates that any symmetrical inspiratory waveform will have the same MDT, provided that inspiratory time is constant. The validity of this assumption is supported by that ventilation with square and sine inspiratory waveforms give rise to the same CO₂ elimination reflected by equal PaCO₂ (6). Notably, a decelerating or accelerating inspiratory flow pattern will have longer and shorter MDTs, respectively, compared to symmetrical flow waveforms. Different waveforms have been studied in man with indistinct

results (6, 9–12). Such studies merit to be repeated with modern technique.

The effect of a longer T_P on V_{Daw} indicates a movement in the proximal direction of the “distal boundary of dead space” (22). As the total airway cross-section area decreases rapidly with each bronchial generation in the cranial direction (23) the rate of this movement must be expected to decline in a non-linear fashion as was found (Figure 2). The variation in V_{Daw} we observed corresponds to about 0.7 mL/kg body weight, which is not trivial with respect to lung protective strategies. In the clinic, it might be desirable to use high RR. If we allow us to extrapolate MDT to 0.25 s (RR 40, T_P 0%), as shown in Figure 3, $V_{CO_2,T}$ would in comparison to MDT 0.51 drop by about 7% and further increase dead space. This would enhance problems related to hypercapnia when V_T is restricted to 6 mL/kg (1).

The effect of a longer T_P on SLOPE implies a more even P_{CO_2} in lung units, which empty non-synchronously. This can either be due to equilibration between parallel units caused by pendelluft or by equilibration along longitudinally oriented units in terms of distal and more proximal alveoli (24). In principle, one cannot from external global observations differentiate between these models (25). One can only speculate that low peripheral resistance in healthy pigs might prevent significant uneven ventilation between parallel lung units. Time-dependent equilibration between proximal and more distal alveoli offer a more likely explanation. Anyway, the more even alveolar concentration reflected by a lower SLOPE after a long T_P was not so important so as to significantly reduce $V_{CO_2,T}$.

Our results agree with previous findings that a post-inspiratory pause enhances CO_2 elimination (4–8). In the present study we used shortest possible tubing (compliance 0.45 mL/cm H_2O). In spite of that, about 4 mL was redistributed from the tubing to the lung when a post-inspiratory pause was applied. If we had not

corrected $V_{CO_2,T}$ for the increase in V_T , effects of a post-inspiratory pause in itself would have been overestimated. In the clinic, both longer tubing and a larger drop in airway pressure at transition to the pause may cause larger V_T variation. In comparison to previous studies the methodological development is considered to increase the validity and accuracy of the results, which increased the ability to quantify changes in dead space related to modest changes in MDT.

MDT affects gas exchange to such an extent that it may be of importance for optimisation of ventilator setting in severe lung disease. Studies of how variation of MDT affects gas exchange are needed in human subjects in health and in disease. Variation of T_P and different inspiratory waveforms merit to be analysed in such studies.

Acknowledgement

We acknowledge the contribution of Dr. Lars Nordström († 2001) for his inspiration and unpublished ideas behind the concept of MDT.

SUPPORTED BY THE SWEDISH RESEARCH COUNCIL (02872) AND THE SWEDISH HEART-LUNG FOUNDATION.

REFERENCES

1. ARDSnetwork. Ventilation with lower tidal volumes as compared with traditional tidal volumes for acute lung injury and the acute respiratory distress syndrome. *N Engl J Med.* 2000;342:1301–1308.
2. Jonson B, Similowski T, Levy P, Viires N, Pariente R. Expiratory flushing of airways: a method to reduce deadspace ventilation. *Eur Respir J.* 1990;3:1202–1205.
3. De Robertis E, Sigurdsson SE, Drefeldt B, Jonson B. Aspiration of airway dead space. A new method to enhance CO₂ elimination. *Am J Respir Crit Care Med.* 1999;159:728–732.
4. Fuleihan SF, Wilson RS, Pontoppidan H. Effect of mechanical ventilation with end-inspiratory pause on blood-gas exchange. *Anesth Analg.* 1976;55:122–130.
5. Lachmann B, Jonson B, Lindroth M, Robertson B. Modes of artificial ventilation in severe respiratory distress syndrome. Lung function and morphology in rabbits after wash-out of alveolar surfactant. *Crit Care Med.* 1982;10:724–732.
6. Dammann JF, McAslan TC, Maffeo CJ. Optimal flow pattern for mechanical ventilation of the lungs. 2. The effect of a sine versus square wave flow pattern with and without an end-inspiratory pause on patients. *Crit Care Med.* 1978;6:293–310.
7. Wolff G, Brunner J, Weibel W, Bowes C. Alveolar efficiency for CO₂ elimination and series dead space volume, both are affected by the ventilatory pattern. *Applied Cardiopulmonary Pathology.* 1989;2:309–314.
8. Mercat A, Diehl JL, Michard F, Anguel N, Teboul JL, Labrousse J, Richard C. Extending inspiratory time in acute respiratory distress syndrome. *Crit Care Med.* 2001;29:40–44.

9. Johansson H, Löfström JB. Effects on breathing mechanics and gas exchange of different inspiratory gas flow patterns during anaesthesia. *Acta Anaesthesiol Scand.* 1975;19:8–18.
10. Johansson H. Effects on breathing mechanics and gas exchange of different inspiratory gas flow patterns in patients undergoing respirator treatment. *Acta Anaesthesiol Scand.* 1975;19:19–27.
11. Al-Saady N, Bennett ED. Decelerating inspiratory flow waveform improves lung mechanics and gas exchange in patients on intermittent positive-pressure ventilation. *Intensive Care Med.* 1985;11:68–75.
12. Markström A, Hedlund A, Lichtwarck-Aschoff M, Nordgren A, Sjöstrand U. Impact of different inspiratory flow patterns on arterial CO₂- tension. *Ups J Med Sci.* 2000;105:17–29.
13. Beydon L, Uttman L, Rawal R, Jonson B. Effects of positive end-expiratory pressure on dead space and its partitions in acute lung injury. *Intensive Care Med.* 2002;28:1239–1245.
14. Uttman L, Jonson B. Computer-aided ventilator resetting is feasible on the basis of a physiological profile. *Acta Anaesthesiol Scand.* 2002;46:289–296.
15. Svantesson C, Drefeldt B, Jonson B. The static pressure-volume relationship of the respiratory system determined with a computer-controlled ventilator. *Clin Physiol.* 1997;17:419–430.
16. Wolff G, Brunner JX. Series dead space volume assessed as the mean value of a distribution function. *Int J Clin Monit Comput.* 1984;1:177–181.
17. Åström E, Niklason L, Drefeldt B, Bajc M, Jonson B. Partitioning of dead space – a method and reference values in the awake human. *Eur Respir J.* 2000;16:659–664.

18. Wolff G, Brunner J, Weibel W, Bowes C, Muchenberger R, Bertschmann W. Anatomical serial dead space volume; concept and measurement in clinical praxis. *Applied Cardiopulmonary Pathology*. 1989;2:299–307.
19. Farhi LE, Rahn, H. Gas stores of the body and the unsteady state. *J Appl Physiol*. 1955;7:472–484.
20. Taskar V, John J, Larsson A, Wetterberg T, Jonson B. Dynamics of carbon dioxide elimination following ventilator resetting. *Chest*. 1995;108:196–202.
21. Woolcock AJ, Macklem PT. Mechanical factors influencing collateral ventilation in human, dog, and pig lungs. *J Appl Physiol*. 1971;30:99–115.
22. Bowes CL, Richardson JD, Cumming G, Horsfield K. Effect of breathing pattern on gas mixing in a model with asymmetrical alveolar ducts. *J Appl Physiol*. 1985;58:18–26.
23. Weibel ER. *Morphometry of the human lung*. Berlin, Springer Verlag; 1963.
24. Fletcher R. *The single breath test for CO₂*, Thesis. Lund University; 1980.
25. West JB. Causes of carbon dioxide retention in lung disease. *N Engl J Med*. 1971;284:1232–1236.

Effects of PEEP increments can be predicted by computer simulation based on a physiological profile in acute lung injury

LEIF UTTMAN¹, LAURENT BEYDON² AND BJÖRN JONSON¹

¹Dept. of Clinical Physiology, University Hospital, Lund, Sweden

²Dept. of Anaesthesia, University Hospital, Angers, France

Abstract

Objective: To test the hypothesis that computer simulation allows prediction of airway pressures and CO₂ elimination (\dot{V}_{CO_2}) after increments of positive end-expiratory pressure (PEEP) in acute lung injury.

Setting: ICU, University hospital.

Design: Prospective, non-randomised comparative trial.

Patients: Twelve consecutive acute lung injury patients.

Intervention: PEEP increments from 0 to 2.5, 5, 7.5, 10 and 15 cm H₂O.

Measurements and results: A physiological profile comprising values for compliance, respiratory resistance and \dot{V}_{CO_2} as a function of tidal volume was established from a recording of ordinary breaths prior to increments of PEEP. Airway pressures and \dot{V}_{CO_2} were measured 30 s after resetting, pressures also after 10 minutes. Values from simulation of the resetting, based on the profile, were compared to measured values. The profiles indicated vast differences in physiology among the 12 subjects. Errors of simulation of airway pressures were non-significant or trivial up to PEEP levels of 10 cm H₂O (95 % of errors < 3 cm H₂O). After 10 minutes plateau pressure was on average 1.5 cm H₂O lower than 30 s after resetting ($p = 0.03$). At increments to PEEP 7.5, 10 and 15, simulation overestimated \dot{V}_{CO_2} by on average 4, 8 and 11%, respectively ($p < 0.05$) because \dot{V}_{CO_2} 30 s after incrementing PEEP decreased with PEEP ($p < 0.001$).

Conclusion: On the basis of a simple lung model simulation predicted effects of moderate increments of PEEP on airway pressures in patients with complex physiology.

Keywords (MeSH): respiratory dead space, pulmonary gas exchange, respiratory distress syndrome, mechanics, artificial ventilation, models

INTRODUCTION

An important principle for the achievement of lung protective ventilation is to minimise tidal lung collapse and re-expansion [1, 2]. Accordingly, an “optimal PEEP level” [3, 4] has since long been used to protect the lung. Another method is to use a small tidal volume (V_T) allowing some degree of permissive hypercapnia [5–8]. The ventilator and the sick lung comprise a very complex system. Identification of a ventilator setting that in a particular patient is optimal with respect to desired physiological effects is therefore difficult.

In technical areas, simulation is a standard procedure used to foresee effects on a complex physical system of a particular action taken to influence a complex physical system. Furthermore, iterative simulation may be performed in order to identify an action or a combination of actions that will lead to desired effects.

Effects of different patterns of mechanical ventilation have been studied by simulation on the basis of mathematical lung modelling [9]. In order to reach desired physiological effects, it has been suggested that a system for iterative simulation based upon a detailed characterisation of the respiratory system might be of help in resetting the ventilator [10].

In healthy pigs, effects of resetting V_T and respiratory rate (RR) were recently predicted by simulation [11]. The simulations were based upon a simple model of lung mechanics and CO_2 elimination per minute (\dot{V}_{CO_2}). Parameters describing lung physiology were automatically estimated from nearly ordinary breaths.

If all properties of the respiratory system were mathematically defined, it would be possible to predict effects of any respiratory pattern. It has proven possible to study lung physiology in great detail also in critically sick patients [12, 13]. However, studies of e.g. viscoelastic properties require special breathing procedures and complex calculations. In the clinic, frequent resetting may be

indicated. More or less automatic simulation procedures are then needed. Our approach is rather to apply a simple model described by parameters calculated from ordinary breaths. The present study represents an initial step in clinical evaluation of simulation as a tool by which a physician may judge in advance the effects of an intended ventilator resetting.

The main objective of the present study was to test the hypothesis that in acute lung injury the immediate effect of positive end-expiratory pressure (PEEP) increments on airway pressures and \dot{V}_{CO_2} could be predicted by simulation, even on the basis of a simple lung model. A secondary objective was to explore how well this simulation predicted observations made after 10 minutes.

METHODS

Material

The ethics committee approved the protocol and informed consent was obtained from the subjects' next of kin. Twelve consecutive patients ventilated for acute lung injury were studied in stable hemodynamic and respiratory condition (Table 1). For 10 of these patients an analysis of effects of PEEP on dead space has previously been presented [13]. The supine subjects were sedated with fentanyl ($5 \mu\text{g}\cdot\text{kg}^{-1}$ in bolus and then $5 \mu\text{g}\cdot\text{kg}^{-1}\cdot\text{h}^{-1}$) and midazolam ($0.05 \text{mg}\cdot\text{kg}^{-1}$ in bolus and then $0.05 \text{mg}\cdot\text{kg}^{-1}\cdot\text{h}^{-1}$). Paralysis was maintained with pancuronium bromide ($0.10 \text{mg}\cdot\text{kg}^{-1}$ in bolus and then $0.10 \text{mg}\cdot\text{kg}^{-1}\cdot\text{h}^{-1}$). In accordance with our clinical routine a humidifying filter was used. The filter contributed to dead space by 100 mL or on average by 16% of V_T . Baseline ventilator setting was volume-control with constant inspiratory flow, RR $17 \pm 1.7 \text{min}^{-1}$, inspiratory time 33%, post-inspiratory pause 20% and PEEP 0. $F_{I}O_2$ was 1.0. Signals for pressure, flow and CO_2 from the Servo Ventilator 900C and CO_2 Analyzer 930 (Siemens-Elema, Solna, Sweden) were recorded after A/D conversion [14].

TABLE 1. PATIENT CHARACTERISTICS

Subject No.	Age (yr)	Height (cm)	Weight (kg)	Cause of Acute Respiratory Failure	Lung Injury Score [31]	V _T (mL)	RR (breaths·min ⁻¹)	PaO ₂ /F _I O ₂ (mm Hg)	Physiol. Dead space (% of V _T)	Days of ventilation
1	55	170	80	Multiple trauma including chest	2.75	532	18	67	57	1
2	31	173	67	Near drowning	2.75	590	16	72	60	1
3	19	183	78	Hemoptysis	2.50	472	21	81	64	2
4	72	183	76	Cardiogenic edema	1.75	747	16	267	41	16
5	67	172	70	Cardiogenic edema	2.75	678	16	118	62	5
6	74	180	70	Pneumonia	2.50	543	18	53	53	1
7	66	178	72	Aortic dissection, post operative	1.00	702	15	265	42	4
8	27	175	71	Chest trauma	2.00	738	14	70	35	2
9	26	174	67	Pneumonia	2.50	528	18	65	44	10
10	43	172	69	Cirrhosis, oesophageal bleeding	2.50	530	18	166	56	4
11	53	162	60	Cardiogenic edema	2.50	614	18	127	50	10
12	34	177	74	Multiple trauma including chest	2.25	818	16	192	42	19

Protocol

A study comprised two parts (Figure 1). During the first part a recording covered 10 normal breaths before resetting of PEEP and a period of 1 minute thereafter. The increments of PEEP were from 0 to 2.5, 5, 7.5, 10 and 15 cm H₂O. Immediately after each level of PEEP the ventilator was reset to 0 cm H₂O PEEP for 1.5 minutes. The periods of increased PEEP were so short that any perturbation of whole body CO₂ equilibrium was considered unimportant [15]. In the second part, similar increments of PEEP lasted 10 minutes. At each PEEP level the 10 last breaths were recorded. The total duration of a study was about 1.5 hours.

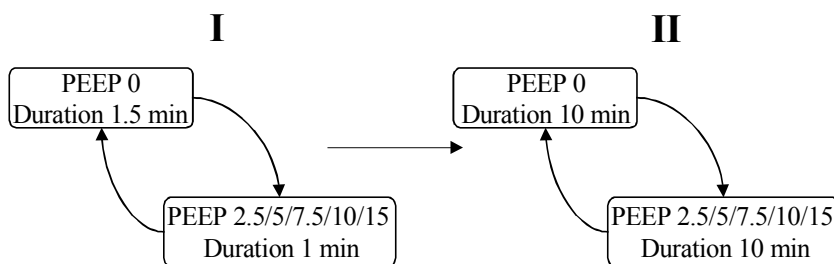


Figure 1. PEEP increments *from* 0 to 2.5, 5, 7.5, 10 and 15 cm H₂O. Resetting of short (I) and long (II) duration.

Data analysis

Coefficients describing the variation of tube resistance with flow according to Rohrer were determined *in vitro* [16]. Tracheal pressure (P_{tr}) was calculated by subtracting the calculated resistive pressure of the tracheal tube from pressure measured in the expiratory circuit of the ventilator [11]. Post-inspiratory elastic recoil pressure (P_{plat}) was read at the end of the 0.7 s long post-inspiratory pause.

The lung model employed constant inspiratory resistance (R_I) and compliance (C) and absence of elastic hysteresis [17, 18]. Compliance was calculated from the slope of P_{tr} versus volume during the period of constant inspiratory flow. When compliance is considered steady this approach is analogous to the method of Ranieri et al. [19]. The trajectory of the elastic recoil pressure (P_{el}) during the breath was then determined from P_{plat} , C and volume (Figure 2). R_I was calculated as the quotient between average $(P_{tr} - P_{el})$ and airway flow rate (\dot{V}_{aw}). Expiratory resistance (R_E) varies with lung volume [17, 20]. The reciprocal of R_E , i.e. expiratory conductance (G_E) was calculated as the quotient between \dot{V}_{aw} and $(P_{tr} - P_{el})$ for each sampling period over the segment covering 15–85% of V_T . The relationship between G_E and volume was determined by linear regression.

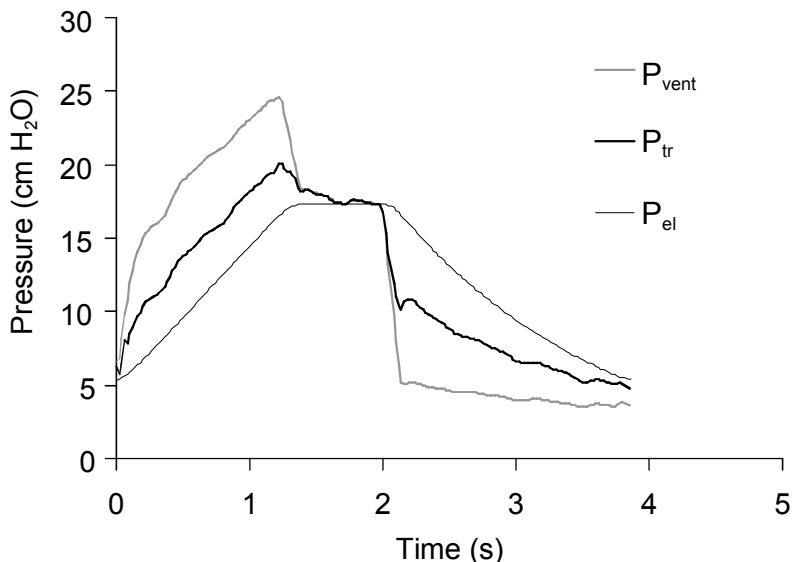


Figure 2. Measured pressure in the expiratory line of the ventilator (P_{vent}), calculated tracheal pressure (P_{tr}) and elastic recoil pressure (P_{el}) during a breath. Total PEEP was estimated as the intercept of the P_{el} curve and the pressure axis.

Signals for \dot{V}_{aw} and CO_2 were analysed to yield the single breath test for CO_2 (SBT- CO_2) according to Fletcher et al. [21]. Tidal CO_2 elimination ($V_{\text{CO}_2,\text{T}}$) reflects the difference between the volume of CO_2 expired ($V_{\text{CO}_2,\text{E}}$) and the volume of CO_2 re-inspired at the start of inspiration ($V_{\text{CO}_2,\text{I}}$) [11]. Parameters describing inspiratory and expiratory resistance, compliance and $V_{\text{CO}_2,\text{T}}$ as a function of V_{T} represent the physiological profile of the subject.

Simulation of an alternative PEEP setting

Immediately before each increment of PEEP, 10 breaths at PEEP 0 were recorded and analysed to provide an update of the physiological profile. Input parameters describing ventilator setting were RR, minute volume, PEEP, inspiratory time and post-inspiratory pause as percent of the respiratory cycle. For inspirations, the performance of the ventilator in the volume-controlled mode was simulated by calculating the effects of a constant flow rate. For expirations, the ventilator's control of PEEP was simulated [11]. Briefly, the physical consequences of ventilator performance were simulated for 6 breaths. Time intervals were 0.02 s or at flow reversals shorter. When R_E tended to decrease during expiration at PEEP 0, R_E was in simulations limited to the value calculated for a volume equal to V_{T} . \dot{V}_{CO_2} was simulated as the product of $V_{\text{CO}_2,\text{T}}$ and RR calculated for the alternative setting. This calculation takes into account changes in both $V_{\text{CO}_2,\text{E}}$ and $V_{\text{CO}_2,\text{I}}$, resulting from changes in V_{T} as previously described [11]. When PEEP was changed, only unintentional minor changes in V_{T} occurred. As the simulation protocol is intended for wider use, the simulation of \dot{V}_{CO_2} as a function of V_{T} was preserved.

Simulation based on the updated physiological profile at PEEP 0 was performed to predict P_{peak} , P_{plat} , mean P_{tr} ($P_{\text{tr,mean}}$) and \dot{V}_{CO_2} after resetting. Median values of up to 10 breaths recorded from 30–60 s after resetting were compared to values from the last simulated breath.

Statistical methods

Data are presented as mean \pm SD. Two-way ANOVA was used to analyse systematic variations of simulation errors and other observations. Student's paired two-tailed t-test was used to further analyse differences. Linear regression was used to analyse the relation between compliance and PEEP in each individual. $p < 0.05$ was considered significant.

RESULTS

The physiological profiles observed at PEEP 0 varied widely between subjects (Table 2). Thus, R_i was 2–22 cm H₂O·s·L⁻¹, R_E at mid- V_T ($R_{E,MID}$) 6–33 cm H₂O·s·L⁻¹, C 29–75 mL·cm H₂O⁻¹. In the SBT-CO₂, the end-tidal slope of the alveolar plateau was 0.7–3.0 mm Hg per 100 mL. Expiratory resistance increased during expiration in 8 of 12 patients.

TABLE 2. PHYSIOLOGICAL PROFILES AT STUDY START

Subject No.	Compliance (mL·cm H ₂ O ⁻¹)	R_i (cm H ₂ O·s·L ⁻¹)	$R_{E,MID}$ (cm H ₂ O·s·L ⁻¹)	$\dot{V}CO_2$ (mL·min ⁻¹)	Alveolar slope (mm Hg·100 mL ⁻¹)
1	39	5	26	272	1.49
2	35	13	21	290	2.26
3	32	22	33	242	2.64
4	42	6	9	263	0.96
5	38	6	6	366	1.85
6	40	3	6	215	1.43
7	42	2	13	323	1.56
8	75	14	32	330	0.77
9	31	6	10	344	0.69
10	37	12	19	359	2.96
11	29	11	27	298	1.25
12	36	8	14	438	1.16

Simulation reached steady state already after 3 of 6 simulated breaths in each case. Differences were observed between measured and simulated loops depicting P_{vent}/V , P_{tr}/V and P_{el}/V (Figure 3).

Thirty seconds after resetting the increase of P_{peak} , P_{plat} and $P_{tr,mean}$ was about 50% of PEEP increments of 2.5 and 5 cm H₂O and increased significantly to about 90% of the PEEP increment of 15 cm H₂O, as further illustrated in Figure 4. The plateau pressure observed at a PEEP of 15 cm H₂O was 39 cm H₂O (range 32–47).

Differences between P_{peak} , P_{plat} , $P_{tr,mean}$ measured 30 s after an increment of PEEP and simulated pressure, represent errors of simulation. These errors were non-significant or trivial up to PEEP levels of 10 cm H₂O (Figure 5). At PEEP 15 cm H₂O, simulation significantly underestimated P_{peak} , P_{plat} , $P_{tr,mean}$ by on average 3.7, 3.9, 1.5 cm H₂O, respectively. The scatter of the error was highest after an increment of PEEP from 0 to 15 cm H₂O. In each patient, compliance decreased significantly with increasing PEEP ($p < 0.05$). When PEEP was increased from 0 to 15 cm H₂O compliance fell by 11–45%.

In order to understand why simulations showed small errors in spite of the fall in compliance, we analysed P_{el} at transitions between expiration and inspiration, which corresponds to total PEEP (PEEP_{tot}). This was done for measured curves (Figure 2) and for simulations. At PEEP 10 simulated PEEP_{tot} was on average 2.2 cm H₂O higher than measured.

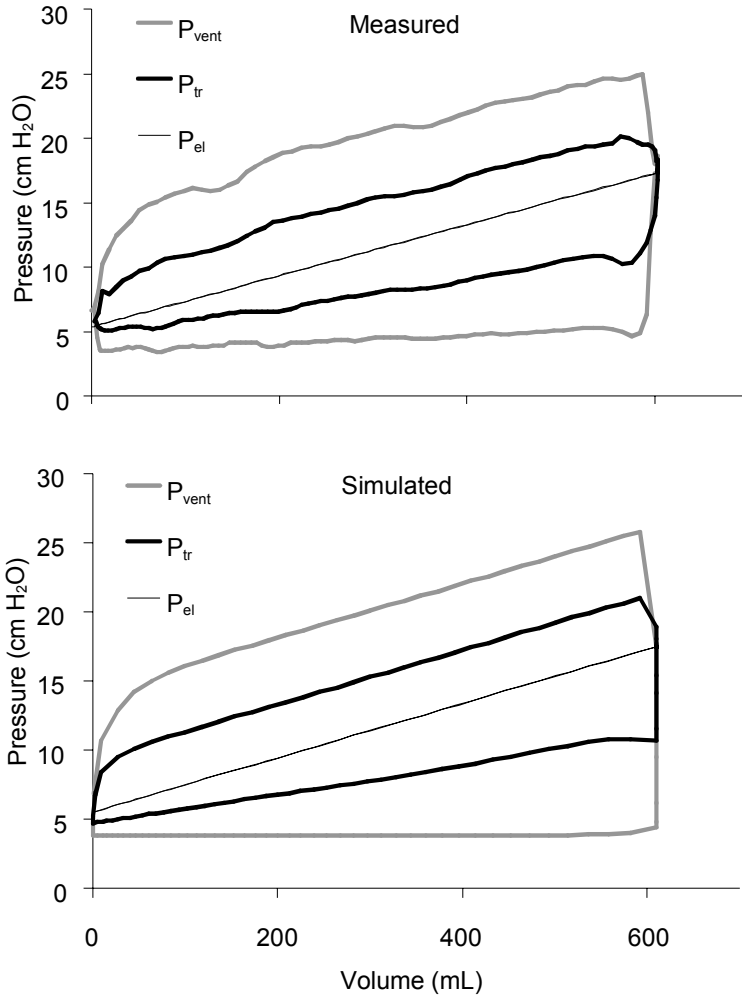


Figure 3. Data from figure 2 presented as pressure/volume loops during a breath depicting measured pressure in the ventilator (P_{vent}), calculated tracheal pressure (P_{tr}) and elastic recoil pressure (P_{el}) (upper panel). Lower panel illustrates the same loops for simulated pressures.

After 10 minutes increments of P_{peak} , P_{plat} , $P_{\text{tr,mean}}$ were less than after 30 s ($p < 0.001$) (Figure 4). The reason for the decline in pressures is a concurrent increase in compliance of on average 4% ($p < 0.001$). This implied that simulated pressures slightly overestimated pressures measured after 10 minutes as shown in Figure 5.

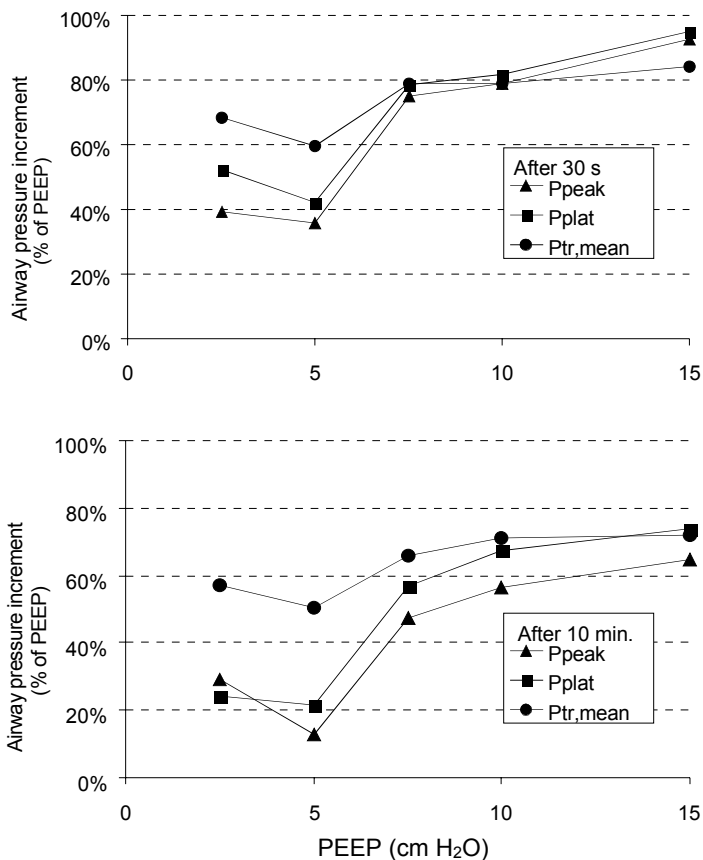


Figure 4. The increase in airway pressures in percent of the PEEP increment measured after 30 s and 10 minutes increased with the level of PEEP (ANOVA, $p < 0.001$).

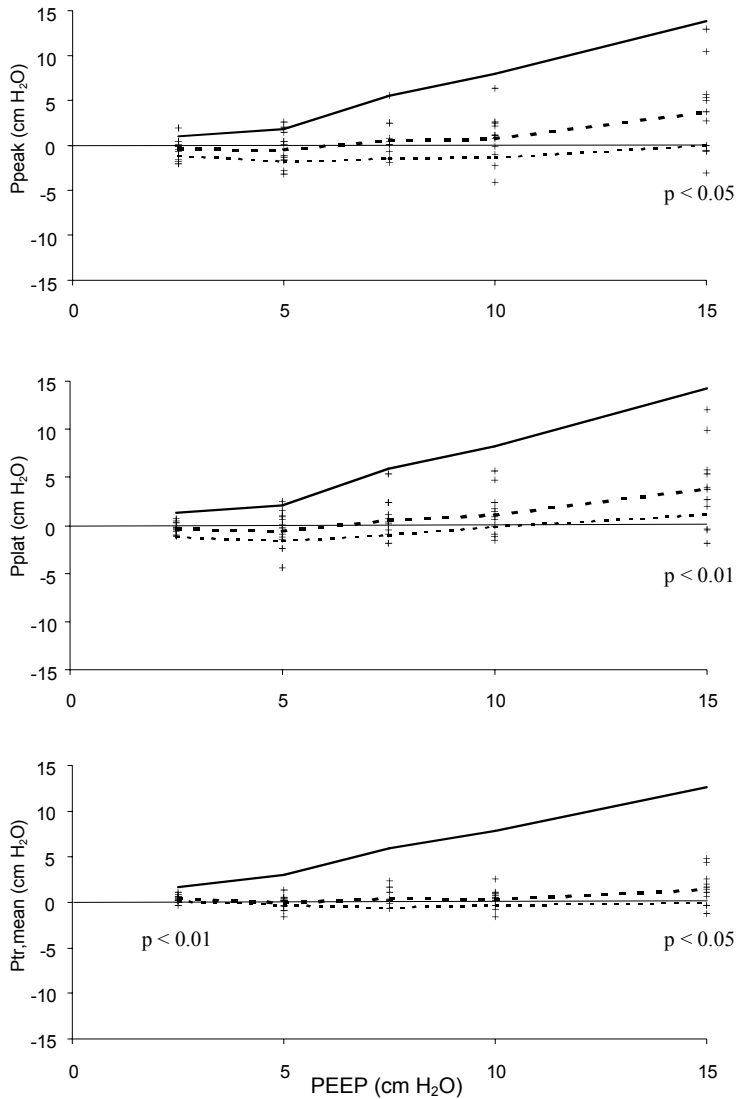


Figure 5. Average observed pressure change after resetting is shown as continuous line, which serves as reference for simulation errors. Average measured minus simulated pressure 30 s after PEEP resetting (simulation error) is shown as heavy interrupted line together with individual errors (+). Average error 10 min after resetting is shown as thin interrupted line. Significant errors for the 30 s resetting are indicated.

\dot{V}_{CO_2} measured 30 s after resetting decreased with increasing PEEP (ANOVA). As a result simulation significantly overestimated \dot{V}_{CO_2} , by on average 4, 8 and 11% when PEEP was increased to 7.5, 10 and 15 cm H₂O, respectively (Figure 6).

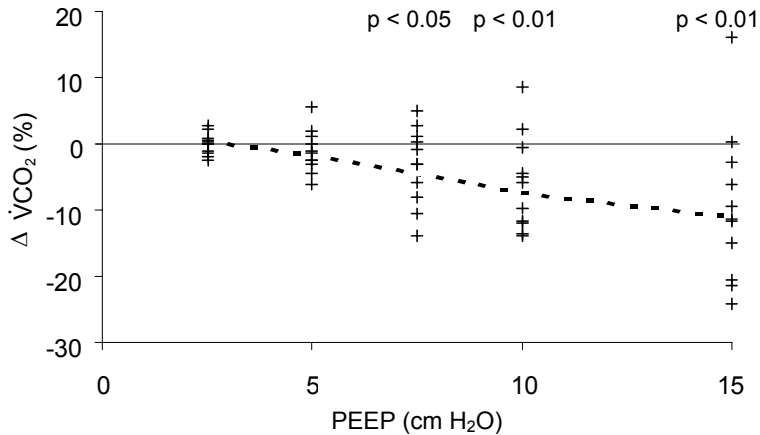


Figure 6. Average measured minus simulated \dot{V}_{CO_2} 30 s after PEEP resetting (simulation error) is shown as heavy interrupted line together with individual errors (+). Significant errors are indicated.

DISCUSSION

In a critically ill patient effects of ventilator resetting on mechanics – in terms of pressure and volume – and on gas exchange need to be considered. This study addresses to what extent effects of PEEP resetting can be predicted by computer simulation.

Oxygenation depends upon several physiological factors, which can be studied bedside only with invasive and complex methods. Examples are cardiac output, right to left shunt and ventilation/perfusion non-homogeneity, which are not easily measured. Furthermore, our knowledge of how ventilator settings affect these factors is too limited to allow simulation of effects on oxygenation of a particular resetting.

We have shown that the SBT-CO₂ allows prediction of how tidal CO₂ elimination changes after resetting of RR and V_T [11]. We used the same system for \dot{V}_{CO_2} simulation to correct for variations in V_T, which in the present study represent random variation. After resetting, \dot{V}_{CO_2} approaches the value representing metabolic CO₂ production [15]. Therefore, \dot{V}_{CO_2} was not analysed after 10 minutes.

A tool for resetting ventilators in intensive care must be simple to use. Mechanics and CO₂ elimination can easily be measured and mathematically described [11]. A manually achieved post-expiratory pause was previously used to measure the post-expiratory elastic recoil pressure. In the present study even this manual operation was eliminated in order to test a principle allowing completely automated establishment of a physiological profile. This lung model includes considerable simplifications. Hysteresis, visco-elasticity, inertia and non-linear elastic properties were disregarded. An issue of the present study was to analyse if these simplifications were compatible with an adequate accuracy of simulations of PEEP resetting. Effects of PEEP on the physiology in acute lung injury further complicate the issue. The volume shifts away from that at PEEP 0, compliance changes and recruitment occurs. To study effects of PEEP among such patients may be regarded as a particularly difficult test situation.

The absence of noise and the use of filtering in the simulation process can explain slightly different features of measured and simulated pressure-volume loops (Figure 3). P_{peak}, P_{plat}, P_{tr,mean} and \dot{V}_{CO_2} were analysed, as these parameters are particularly relevant for lung

protective ventilation [5, 7]. Results in Figure 5 and 6 reflect summation of errors in measurements, modelling and simulation. Errors caused by unstable physiology were minimised as the physiological profile was updated immediately before each PEEP increment.

Changes of pressures after a PEEP increment of 15 cm H₂O were significantly underestimated. The explanation is that the model did not simulate the fall in compliance. For PEEP increments up to 10 cm H₂O such errors were compensated by a fall in PEEP_{tot}, explained by a shorter time constant for the exponentially falling lung volume and therefore a faster emptying of the lungs. The slight decrease of pressures between 30 s and 10 minutes after PEEP increments reflects an increase in compliance that probably indicates recruitment. Simulation was equally useful to predict airway pressures at 10 minutes as well as 30 s after resetting.

The observed decrease in \dot{V}_{CO_2} 30 s after large increments of PEEP may be explained by increased airway dead space [13, 22]. Alternative explanations are PEEP related effects on hemodynamics: Compression of capillaries in open lung regions may cause diversion of blood flow toward collapsed areas [23, 24]. Furthermore, effects of reduced preload and raised juxtacardiac pressure, may result in reduced ventricular filling pressure and a decrease in cardiac output [25, 26]. In a study of 10 out of the present 12 subjects, alveolar dead space did not change with PEEP, leaving PaCO₂ unchanged 10 minutes after PEEP elevation [13]. Therefore, hemodynamic factors are probably not the main cause of the changes in \dot{V}_{CO_2} . If prevailing, a decrease in \dot{V}_{CO_2} would after equilibration lead to an inversely proportional increase in PaCO₂ [15]. However, as no changes of PaCO₂ occurred according to Beydon et al. [13], the change in \dot{V}_{CO_2} causing small simulation errors at modest increments of PEEP shown in Figure 6 would not be of clinical importance. F_IO₂ was 1.0 in order to standardise conditions and secure oxygenation

even at PEEP 0 at which it may have favoured the formation of atelectasis [27]. Especially PEEP 15 may have led to time dependent recruitment [28, 29]. Recruitment may explain the decrease of alveolar dead space observed in some patients in whom PaO_2 increased at higher PEEP [13].

Previously we showed that simulation predicted effects of V_T and RR changes in healthy pigs [11]. In the present study effects of moderate increments of PEEP were foreseen in subjects with acute lung injury according to our hypothesis. Hence, predictions may be based on physiological observations followed by simulation. The simplified lung model prevents prediction of gross changes in ventilator setting. On the other hand, the simple lung model eliminates the need for special measurement procedures and facilitates a stepwise resetting guided by simulation.

Notably, observations are so far limited to sedated and paralysed pigs and a small number of patients. It is foreseen that difficulties are far greater in patients under ventilator support. The high $F_{\text{I}}\text{O}_2$ may have influenced the results. Effects on PEEP_{tot} , which contributed to the fit between measured and simulated pressures, may not be typical for other situations. Accordingly, it is too early to judge if simulation may be clinically useful. The principle must be tested in wide groups of patients and in conjunction with clinically relevant types of resetting. Alternative principles for characterising lung physiology, for example implementation of non-linear elastic properties [19] or parameter estimation by artificial neural network [30] merit to be tested.

Supported by the Swedish Research Council (02872) and the Swedish Heart-Lung Foundation.

REFERENCES

1. Lachmann B, Jonson B, Lindroth M, Robertson B (1982) Modes of artificial ventilation in severe respiratory distress syndrome. Lung function and morphology in rabbits after wash-out of alveolar surfactant. *Crit Care Med* 10:724–732.
2. Jonson B (1982) Positive airway pressure: some physical and biological effects. IN: Prakash O (ed) *Applied physiology in clinical respiratory care*. Martinus Nihoff Publishers BV, The Hague, pp 125–139.
3. Suter PM, Fairley B, Isenberg MD (1975) Optimum end-expiratory airway pressure in patients with acute pulmonary failure. *N Engl J Med* 292:284–289.
4. Landers S, Hansen TN, Corbet AJ, Stevener MJ, Rudolph AJ (1986) Optimal constant positive airway pressure assessed by arterial alveolar difference for CO₂ in hyaline membrane disease. *Pediatr Res* 20:884–889.
5. The Acute Respiratory Distress Syndrome Network (2000) Ventilation with lower tidal volumes as compared with traditional tidal volumes for acute lung injury and the acute respiratory distress syndrome. *N Engl J Med* 342:1301–1308.
6. Mariani G, Cifuentes J, Carlo WA (1999) Randomized trial of permissive hypercapnia in preterm infants. *Pediatrics* 104:1082–1088.
7. Amato MB, Barbas CS, Medeiros DM, Magaldi RB, Schettino GP, Lorenzi-Filho GKRA, Deheinzelin D, Munoz C, Oliveira R, Takagaki TY, Carvalho CR (1998) Effect of protective-ventilation strategy on mortality in the acute respiratory distress syndrome. *N Engl J Med* 338:347–354.
8. Amato MB, Barbas CS, Medeiros DM, Schettino G, Lorenzi FG, Kairalla RA, Deheinzelin D, Morais C, Fernandes E, Takagaki TY (1995) Beneficial effects of the “open lung approach” with low distending pressures in acute respiratory distress syndrome. A prospective randomized study on mechanical ventilation. *Am J Respir Crit Care Med* 152:1835–1846.

9. Jansson L and Jonson B (1972) A theoretical study on flow patterns of ventilators. *Scand J Respir Dis* 53:237–246.
10. Uttman L, Sigurdsson S, Jonson B (1999) Computer simulation: a guideline in ventilator setting in severe lung disease. *Crit Care* 3:Suppl.1:A37.
11. Uttman L and Jonson B (2002) Computer-aided ventilator resetting is feasible on the basis of a physiological profile. *Acta Anaesthesiol Scand* 46:289–296.
12. Jonson B, Richard JC, Straus C, Mancebo J, Lemaire F, Brochard L (1999) Pressure-volume curves and compliance in acute lung injury: evidence of recruitment above the lower inflection point. *Am J Respir Crit Care Med* 159:1172–1178.
13. Beydon L, Uttman L, Rawal R, Jonson B (2002) Effects of positive end-expiratory pressure on dead space and its partitions in acute lung injury. *Intensive Care Med* 28:1239–1245.
14. Svantesson C, Drefeldt B, Jonson B (1997) The static pressure-volume relationship of the respiratory system determined with a computer-controlled ventilator. *Clinical Physiology* 17:419–430.
15. Taskar V, John J, Larsson A, Wetterberg T, Jonson B (1995) Dynamics of carbon dioxide elimination following ventilator resetting. *Chest* 108:196–202.
16. Rohrer F (1915) Der Strömungswiderstand in den menschlichen Atemwegen und der Einfluss der unregelmässigen Verzweigung des Bronchialsystems auf den Atmungsverlauf. *Archiv für die gesamte Physiologie* 162:225–299.
17. Jonson B, Beydon L, Brauer K, Månsson C, Valind S, Grytzell H (1993) Mechanics of respiratory system in healthy anesthetized humans with emphasis on viscoelastic properties. *J Appl Physiol* 75:132–140.
18. Beydon L, Svantesson C, Brauer K, Lemaire F, Jonson B (1996) Respiratory mechanics in patients ventilated for critical lung disease. *Eur Respir J* 9:262–273.

19. Ranieri VM, Zhang H, Mascia L, Aubin M, Lin CY, Mullen JB, Grasso S, Binnie M, Volgyesi GA, Eng P, Slutsky AS (2000) Pressure-time curve predicts minimally injurious ventilatory strategy in an isolated rat lung model. *Anesthesiology* 93:1320–1328.
20. Briscoe WA and Dubois AB (1958) The relationship between airway resistance, airway conductance and lung volume in subjects of different age and body size. *J Clin Invest* 37:1279–1285.
21. Fletcher R, Jonson B, Cumming G, Brew J (1981) The concept of dead space with special reference to the single breath test for carbon dioxide. *Br J Anaesth* 53:77–88.
22. Larsson A, Gilbert JT, Bunegin L, Gelineau J, Smith RB (1992) Pulmonary effects of body position, PEEP, and surfactant depletion in dogs. *Acta Anaesthesiol Scand* 36:38–45.
23. Nieman GF, Paskanik AM, Bredenberg CE (1988) Effect of positive end-expiratory pressure on alveolar capillary perfusion. *J Thorac Cardiovasc Surg* 95:712–716.
24. Kanarek DJ and Shannon DC (1975) Adverse effect of positive end-expiratory pressure on pulmonary perfusion and arterial oxygenation. *Am Rev Respir Dis* 112:457–459.
25. Marini JJ, Culver BH, Butler J (1981) Effect of positive end-expiratory pressure on canine ventricular function curves. *J Appl Physiol* 51:1367–1374.
26. Potkin RT, Hudson LD, Weaver LJ, Trobaugh G (1987) Effect of positive end-expiratory pressure on right and left ventricular function in patients with the adult respiratory distress syndrome. *Am Rev Respir Dis* 135:307–311.
27. Rothen HU, Sporre B, Engberg G, Wegenius G, Reber A, Hedenstierna G (1995) Prevention of atelectasis during general anaesthesia. *Lancet* 345:1387–1391.

28. Neumann P, Rothen HU, Berglund JE, Valtysson J, Magnusson A, Hedenstierna G (1999) Positive end-expiratory pressure prevents atelectasis during general anaesthesia even in the presence of a high inspired oxygen concentration. *Acta Anaesthesiol Scand* 43:295–301.
29. Richard JC, Maggiore SM, Jonson B, Mancebo J, Lemaire F, Brochard L (2001) Influence of tidal volume on alveolar recruitment. Respective role of PEEP and a recruitment maneuver. *Am J Respir Crit Care Med* 163:1609–1613.
30. Perchiazzi G, Högman M, Rylander C, Giuliani R, Fiore T, Hedenstierna G (2001) Assessment of respiratory system mechanics by artificial neural networks: an exploratory study. *J Appl Physiol* 90:1817–1824.
31. Murray JF, Matthay MA, Luce JM, Flick MR (1988) An expanded definition of the adult respiratory distress syndrome. *Am Rev Respir Dis* 138:720–723.

